

The old moving groups in the field of Taurus

JIAMING LIU,¹ MIN FANG,² HAO TIAN,³ CHAO LIU,^{3,4} CHENGQUN YANG,⁵ AND XIANGXIANG XUE¹

¹*Key Laboratory of Optical Astronomy, National Astronomical Observatories, Chinese Academy of Sciences, Beijing 100101, China*

²*Purple Mountain Observatory, Chinese Academy of Sciences, 10 Yuanhua Road, Nanjing 210023, China*

³*Key Lab of Space Astronomy and Technology, National Astronomical Observatories, CAS, Beijing, 100101, China*

⁴*University of Chinese Academy of Sciences, Beijing 100049, China*

⁵*Shanghai Astronomical Observatory, 80 Nandan Road, Shanghai 200030, People's Republic of China*

(Received XXX; Revised XXX; Accepted XXX)

Submitted to ApJs

ABSTRACT

In this work, we present a systematic search for stellar groups in the Taurus field by applying DBSCAN algorithm to the data from *Gaia* DR2. We find 22 groups, consisting of 8 young groups (Groups 1–8) at ages of 2–4 Myr and distances of ~ 130 –170 pc, 14 old groups (Groups 9–22) at ages of 8–49 Myr and distances of ~ 110 –210 pc. We characterize the disk properties of group members and find 19 new disk-bearing stars, 8 of which are in the young groups and 11 others belong to the comparatively old groups at ages of 8–11 Myr. We characterize the accretion properties of the group members with H α emission line in their LAMOST spectra, and discover one source in Group 10 at an age of 10 Myr which still shows accretion activity. We investigate the kinematic relations among the old groups, and find that Group 9 is kinematically related to the known Taurus members and exclude any kinematic relations between Groups 10–22 and the known Taurus members.

Keywords: Accretion: stallar accretion: stellar accretion disks-Stars: pre-main-sequence-Star clusters: stellar associations-star formation: star formation regions

1. INTRODUCTION

Taurus is one of the most famous nearby (130–160 pc, Torres et al. 2009) star forming region. This region has been surveyed with various telescopes at different wavelengths, e.g. the infrared imaging survey with the IRAS, Spitzer, and WISE telescopes (Kenyon et al. 1990; Luhman et al. 2010; Rebull et al. 2010, 2011; Esplin et al. 2014), the optical imaging survey (Briceño et al. 2002; Slesnick et al. 2006), the UV imaging survey with the GALEX (Findeisen & Hillenbrand 2010; Gómez de Castro et al. 2015), the X-ray survey with the XMM-Newton telescope (Güdel et al. 2007). These surveys identified ~ 400 young stars and brown dwarfs over a sky coverage of more than 100 deg² in Taurus region (Luhman et al. 2010; Rebull et al. 2010).

In Taurus, the known young stellar objects (YSOs) tend to group within active star forming regions with dense molecular clouds (Briceño et al. 2002; Luhman 2004; Luhman et al. 2009; Esplin & Luhman 2017). With the astrometric data of *Gaia* DR2, Luhman (2018) found that these young stars can be grouped into four populations (i.e. Populations red, blue, green and cyan, see Figure 1). The latest catalogue for the members in Taurus is from Esplin & Luhman (2019), in which 519 sources are listed. With the latest catalogue, Roccatagliata et al. (2020) also studied the grouping of young stars in Taurus, and conclude that the members can be well divided into 6 populations (Figure 1) with different distances and kinematics, indicating a complex star formation in this region. Besides the young populations in Taurus, it has been known that there are "old" populations with ages of ~ 10 Myrs distributed in the field of Taurus (Slesnick et al. 2006; Kraus et al. 2017; Zhang et al. 2018). Luhman (2018) examine the kinematics and parallaxes of these "old" populations and conclude

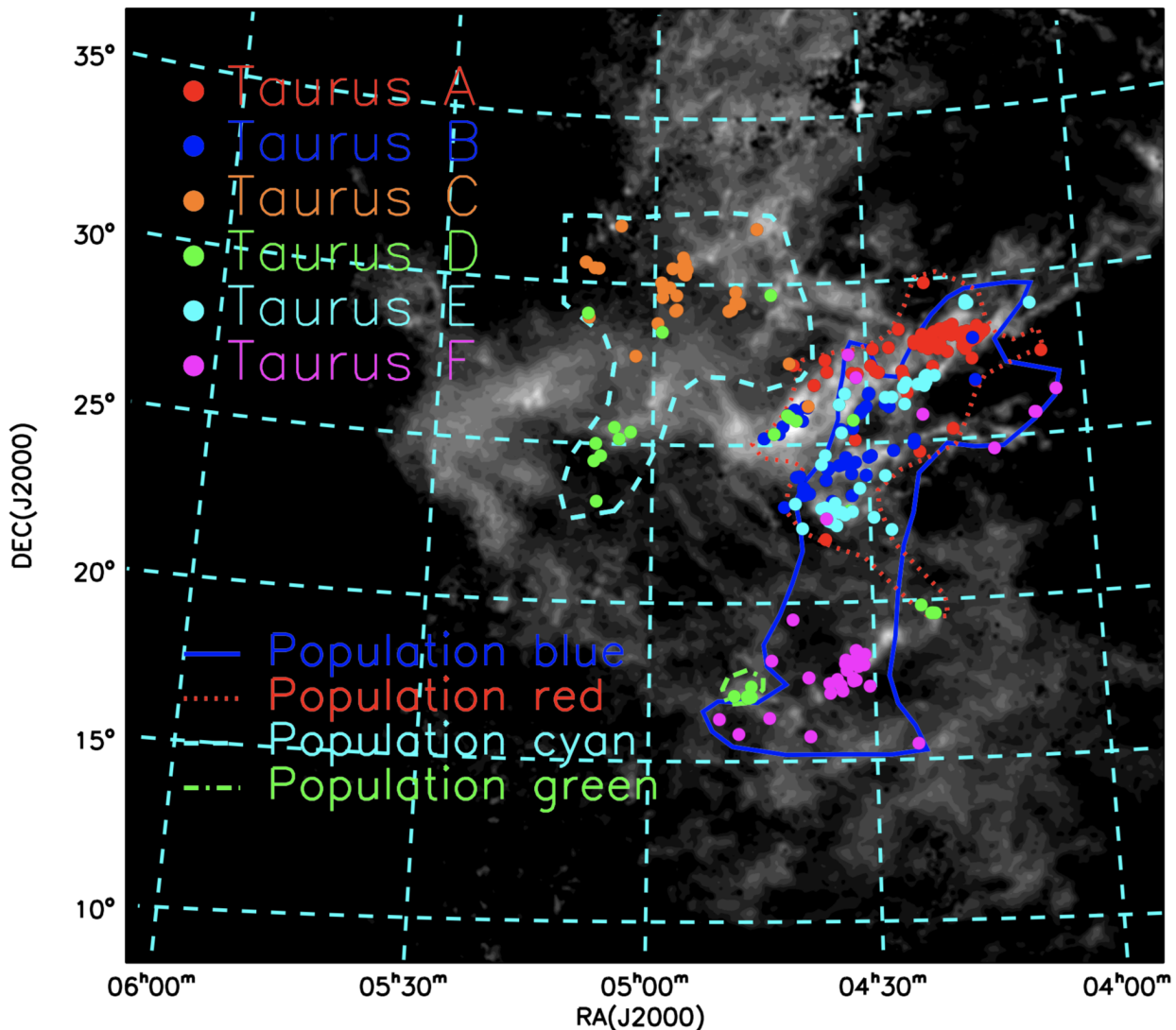


Figure 1. The Taurus region and the previously identified YSO groups. Solid dots with different colors denote the distributions of the YSO groups of Roccatagliata et al. (2020), while the lines coded with different colors are the locations of the YSO groups defined by Luhman (2018). Background image are the cumulative extinction map of Green et al. (2019) to 300 pc.

that most of them are not associated with the young populations in Taurus.

The previous studies on the stellar groups in the Taurus field mostly focused on the known young members, and a systematic search for stellar groups of older ages have not been performed. These groups could be relevant or irrelevant to Taurus star-forming regions and the known YSOs, and could improve our understanding of star formation history in the field of Taurus (not necessarily associated with the Taurus star-forming regions). In considering of this, we carry out an extensive search for the stellar groups in the field of Taurus using the *Gaia* DR2 astrometric data. We organized the work as follows: we will describe data in § 2, and delineate the data analysis in § 3. We will present the results in § 4,

followed by a discussion in § 5, and a summary of the work in § 6.

2. DATA

In order to fully explore the Taurus region, we use a large searching area: $55^\circ < \text{RA} \leq 90^\circ$ and $10^\circ \leq \text{DEC} \leq 35^\circ$. Within this area, we extract the stars with signal-to-noise ratios in parallax larger than 5 ($\varpi/\sigma_\varpi \geq 5$). We only select the sources with the parallaxes between 3.33 and 10 mas, corresponding to 100-300 pc, in order to search for the groups with distance near the Taurus star forming region. In the northwest of Taurus, there is another star forming region, Perseus. We remove this region from the study in this work by excluding the sources within the area of $55^\circ \leq \text{RA} \leq 70^\circ$ and $30^\circ \leq \text{DEC} \leq 35^\circ$. In our studied area, there is

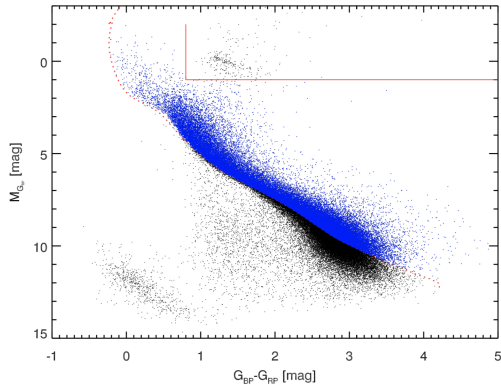


Figure 2. The 100 Myr cut to eliminate the field main sequence stars. The red dotted line indicate the 100 Myr isochrone of PARSEC. The red solid line indicates the selection region, and blue dots denote stars selected in this 100 Myr cut.

also a known open cluster, Melotte 22. This cluster is easily identified in the space of proper motions (centered at $\mu_\alpha \sim 20$ mas/yr and $\mu_\delta \sim -45$ mas/yr, Lodieu et al. (2019)). In this work, we limit μ_δ between -40 and -10 mas/yr in order to (1) search for the potentially co-moving groups with Taurus and (2) exclude the Melotte 22 cluster from our sample. We are interested in searching for the young groups. To achieve this, we employ a color-magnitude diagram using the photometry from *Gaia* DR2 (see Figure 2). We require that all the sources used in this work must be above the 100 Myr isochrone from Bressan et al. (2012). As noted in Figure 2, there are a group of post-main sequence stars at the top-right side of the color-magnitude diagram. In order to remove them, we exclude the sources with $M_{GRP} < 1$ and $G_{BP} - G_{RP} > 0.8$. The color-magnitude diagram shown in Figure 2 is not dereddened, then our selected sample could include some highly reddened old stars. Thus, it is important to evaluate the reddening of individual sources which will be done later for the interesting objects, see §3.3.

2.1. Spectra data

The spectroscopic data used in this work are taken from LAMOST DR5. LAMOST (The Large Sky Area Multi-Object Fibre Spectroscopic Telescope) is a 4m Schmidt telescope of the National Astronomical Observatories of China (NAOC), located at Xinglong Observing Station, China. With 4000 fibers on board the focus, LAMOST can observe nearly 4000 spectra simultaneously in optical bands of $\sim 3900 - 9000$ Å, at a resolution of ~ 1800 (Cui et al. 2012). In this work, we use the LAMOST DR5 dataset.

2.2. Photometric data

In order to construct the spectral energy distribution of each source and estimate its extinction, we used optical photometry in the g , r , i , z , and y bands from Pan-STARRS (Chambers et al. 2016) and G , G_{BP} , and G_{RP} bands from *Gaia* DR2 (Gaia Collaboration et al. 2016, 2017, 2018), near-infrared photometry in the J , H , and K_S bands from the Two-Micron All Sky Survey (2MASS, Skrutskie et al. 2006), near- and mid-infrared photometry in the $W1$ ($3.4 \mu\text{m}$), $W2$ ($4.6 \mu\text{m}$), $W3$ ($12 \mu\text{m}$) and $W4$ ($22 \mu\text{m}$) bands from WISE (Wright et al. 2010, The Wide-field Infrared Survey Explorer) allsky survey.

3. GROUP SEARCHING AND ANALYSIS

3.1. Method: DBSCAN

In this work, We use DBSCAN to search groups in the Taurus field. DBSCAN is a density-based clustering method. Its principal idea is if a point is belonging to a group, then it should be surrounded by members of the same group in the multi-dimensional space. The idea is realized by finding neighborhoods of data points exceed a given density threshold, which is defined as the minimum number of neighbors or data points ($minPts$) within a given search radius (ϵ). The algorithm can be summarized as:

1. With the given threshold ($minPts$ and ϵ), starting from a random data point, the code will find all the points inside the radius ϵ (e.g. neighbourhoods of the data point). If the number of data points is greater than $minPts$, then all these data points will be regarded as a part of a “cluster”.
2. From each of these data points identified in Step 1, the code will repeat the step 1 to search for new data points upon the defined threshold above until no more new data points can be found. All the data points found in this step are also regarded as members of the cluster revealed in Step 1.

For DBSCAN, large $minPts$ values and small ϵ values are sensitive to those highly concentrated parts of the stellar groups, and on the contrary small $minPts$ and large ϵ values will include too much contamination from field stars, and mis-recognize groups. In this work, we perform the DBSCAN algorithm with the python package Sklearn of Pedregosa et al. (2012) to a 5 dimensional normalized astrometric space that consists of x , y , z , μ'_α and μ'_δ , where x , y , and z are in cartesian space, μ'_α and μ'_δ refer to the tangential velocities in the right ascen-

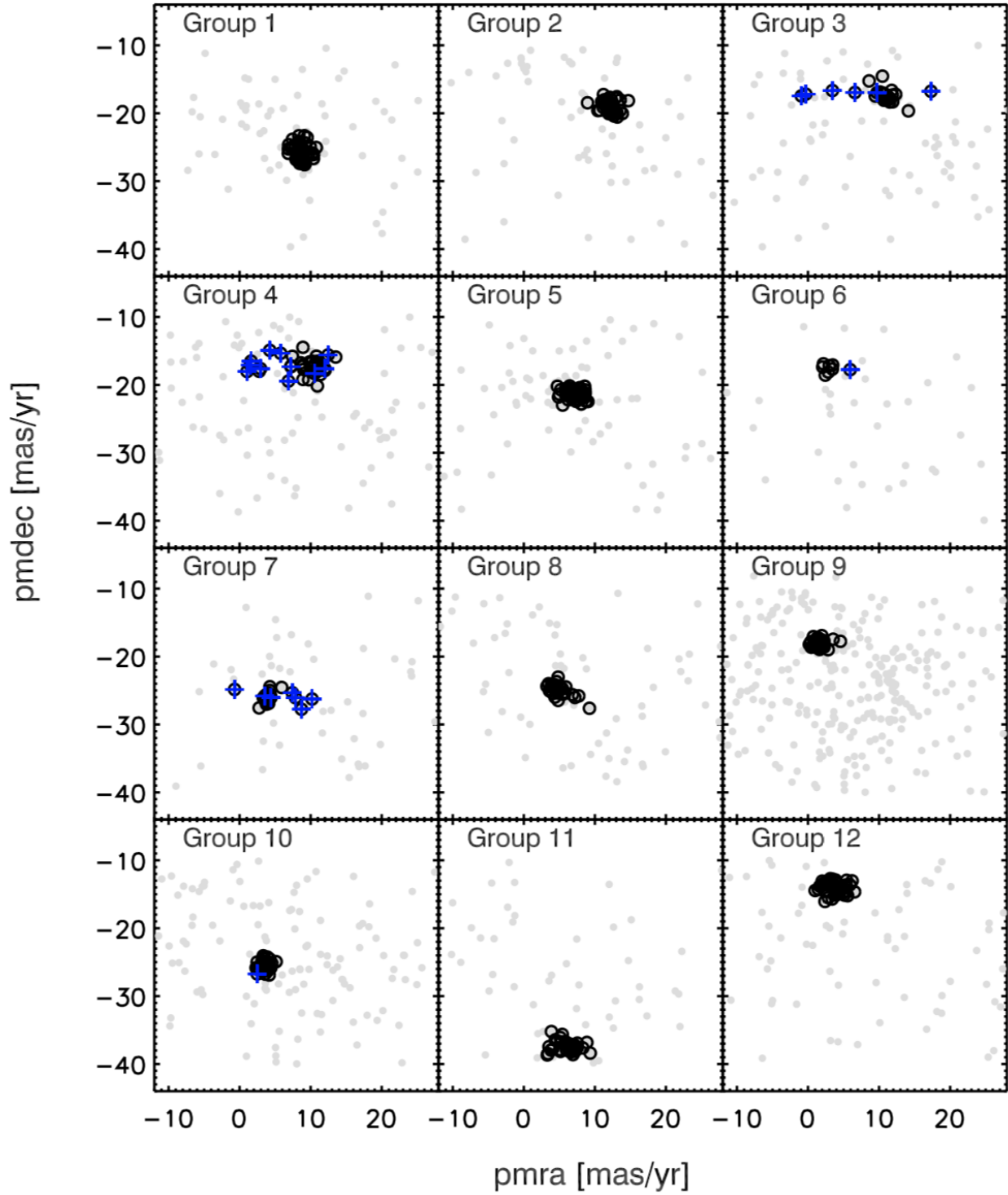


Figure 3. The clustering of the identified groups 1–12 in the proper motion spaces. Gray solid dots are the surrounding stars within 15 pc from the center of each individual group, while black open circles mark group members located by DBSCAN. Note that in each panel we only include one group, and the members of other groups have been removed. The blue crosses mark the nonmembers that ruled out by CMD (see section 4.1).

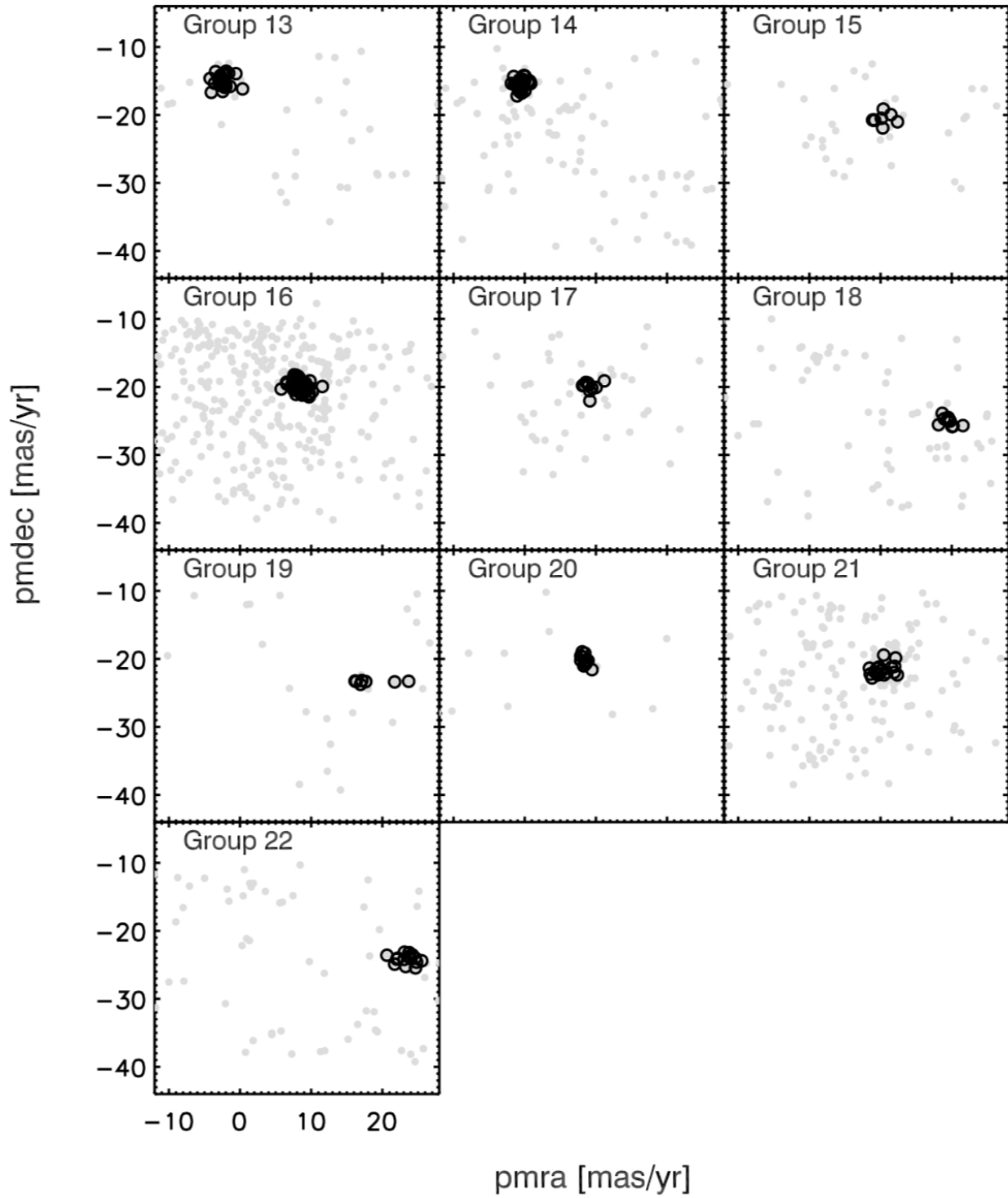


Figure 4. Same as figure 3 but for Groups 13–22.

sion and declination direction ¹. We vary $minPts$ from 5 to 15, and ϵ from 0.01 to 0.1 to look for the reasonable values which can re-discover the YSO groups identified in Taurus. Roccatagliata et al. (2020) perform a group search among the spectroscopically confirmed members in Taurus, and find six populations, Groups A–F, with well defined parallax and proper motions. We find that by setting $minPts = 9$ and $\epsilon = 0.035$, the DBSCAN algorithm can re-discover these groups. With $minPts = 9$ and $\epsilon = 0.035$, the DBSCAN algorithm find 22 groups in the whole region. However, we must stress that our group searching could ignore smaller and more sparse groups than the YSO groups since we have set the $minPts$ and ϵ to be efficient for searching the YSO groups.

In order to minimize the influence of the projection effect and to remove the contamination in the group member from the field stars, we further refine the result in the above using a more rigorous criteria via two steps:

1. For each group, we apply the DBSCAN algorithm to the stars within 15 pc from the center of the group by setting $minPts=9$ and varying ϵ between 0.1 and 0.2. The normalization scale in this step is much smaller than the above one, and the ϵ used here is corresponding to 0.015 to 0.03 if using the same normalization scale as the above. In this step, we relatively reduce the search radius (smaller ϵ) to mitigate the contamination in the group members from field stars. However, we could lose some members which are far from the group center.
2. For each group, we only include the sources with proper motions within 2σ from the mean proper motions of the group (see Figure 3 and 4), where σ is the standard deviation of the proper motions for the member candidates of the group.

During the refinements, we have excluded about one hundred sources from our preliminary sample. Finally, we have 630 sources in our refined sample that are grouped into 22 populations (see Figure 5 for their distribution in the sky). The standard deviation of these groups in the tangential velocity space is $\sim 0.73 \text{ km}^{-1}$. As a comparison, We derive the the median value ($\sim 2.33 \text{ km}^{-1}$) of the standard deviations of tangential velocities derived from the stellar associations in Gagné

¹ For each parameter p of the 5 dimensional space, the normalization is done as: $p_n = (p_i - p_{min}) / (p_{max} - p_{min})$, where p_{max} and p_{min} are the maximum and minimum value of i -th parameter p_i .

et al. 2018a using Gaia DR2 data. This indicates that our group method is very conservative and should have lost some group members. We will further refine their members of individual groups based on their locations in the dereddened M_{GRP} vs $G_{BP} - G_{RP}$ diagrams (see Section 4.1).

We must stress that the group result could be influenced by the projection effect. It would be more reliable for searching stellar groups if using the x, y, z, U, V, W spaces, where U, V, W velocities are the velocities in the x, y, z directions respectively. However, it will severely cut down the number of stars as only bright stars ($G \geq 13.0$) are released with radial velocities in Gaia DR2.

3.2. spectral types

We match the member candidates of each group with the known young stars with spectral types in the literature with a $2''$ matching radius, and find 298 ones (Slesnick et al. 2006; Kraus et al. 2017; Esplin & Luhman 2019; Cannon & Pickering 1993; Nesterov et al. 1995; Biazzo et al. 2012; Herczeg & Hillenbrand 2014; Gagné et al. 2018b; Kervella et al. 2019). We also search for the spectra of our targets in LAMOST DR5, and retrieve the spectral data for 267 ones. Among them, 48 have been classified with the LAMOST pipeline, and the results are used in this work. For the other 219 sources without the spectral types from the LAMOST DR5, we classify their spectra with the method described in Fang et al. (2017). To evaluate the reliability of our spectral classification, we compared the spectral types of the 106 common sources with spectral type derived in this work and in the literature (Wichmann et al. 1996; Slesnick et al. 2006; Kraus et al. 2017; Luhman 2018), see Figure 6. The comparison shows there is no systematic difference between the spectral types in the literature and in this work. We note that two sources, BP Tau and HO Tau, show more than 2σ difference on the spectral types. The large difference on the spectral types for an accreting young star is very common, and can be due to variable optical veiling on the spectra (Fang et al. 2020a), since the spectral classification usually does not consider veiling effect.

In total, we have spectral types for 427 sources in our sample, and 298 ones from literature and 129 derived from the LAMOST spectra.

3.3. Extinction

Our sample contains about three hundreds well studied young stars in Taurus, and their published extinction are adopted in this work (Herczeg & Hillenbrand 2014; Esplin & Luhman 2019). For those without estimates

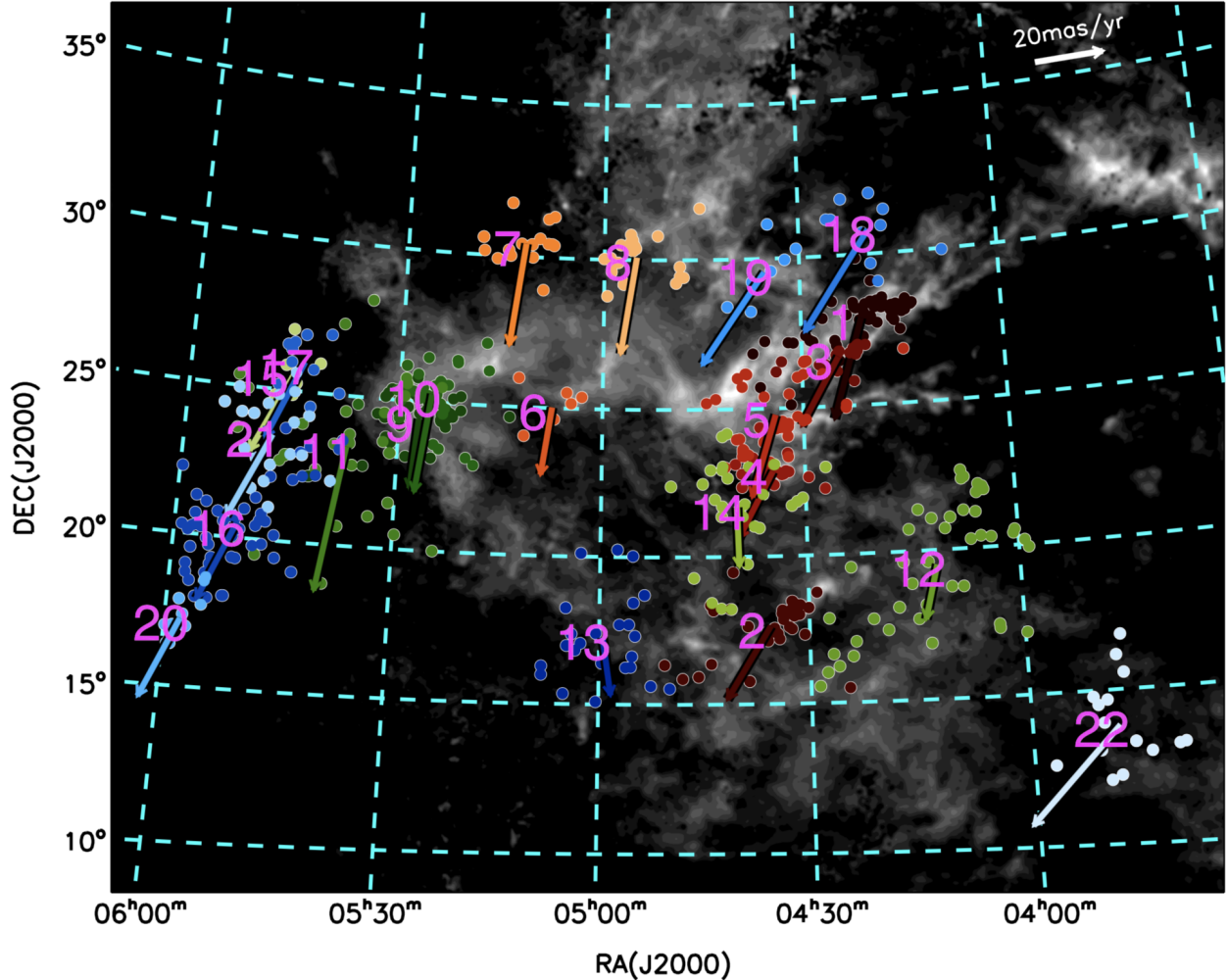


Figure 5. Stellar groups identified in this work over plotted on the cumulative extinction map of Green et al. (2019) to 300 pc. Each group is shown as different colors. The average proper motion for each group are show as arrows in the figure.

of extinction in the literature, we derive their extinctions. For the ones with spectral types, we convert their spectral types to effective temperatures (T_{eff}) using the conversions in Fang et al. (2017), which are from Pecaut & Mamajek (2013) for stars earlier than M4 and from Herczeg & Hillenbrand (2014) for stars later than M4 type. We then achieve their intrinsic colors for $G_{RP} - J$ corresponding to their T_{eff} by interpolating the model colors for the 10 Myr isochrone from PARSEC (Bressan et al. 2012), and derive the extinction of individual sources using the average extinction law with the total-to-selective extinction ratio $R_V = 3.1$ from Wang and Chen (2019). We verify this method by comparing our results with those in Herczeg & Hillenbrand (2014) for the common sources. The comparison shows that both agree well with each other, see the left panel in Figure 7.

For the sources without spectral types, we perform a least-square fit to the observed colors, taking the extinc-

tion and T_{eff} as free parameters. The colors used in the fitting are a combination of the broad-band photometry in *Gaia* G_{BP} , G_{RP} bands and 2MASS J , H , K_s bands. For each T_{eff} we obtain the model colors for the 10 Myr isochrone from PARSEC (Bressan et al. 2012), redden them using the same extinction law with $R_V = 3.1$ from Wang and Chen (2019), and then compare the reddened colors to the observed ones. The best-fit to the observed colors yields the extinction used in this work. The extinctions derived in this method are mostly for the diskless sources. To verify this method, we collect a sample of the sources with spectral types in the old groups and estimate their extinctions using the above two methods. We compare the extinctions from the two methods in the right panel in Figure 7, which shows a good agreement between them.

We further verify our derived extinction by repeating the above procedure by using the model colors for the

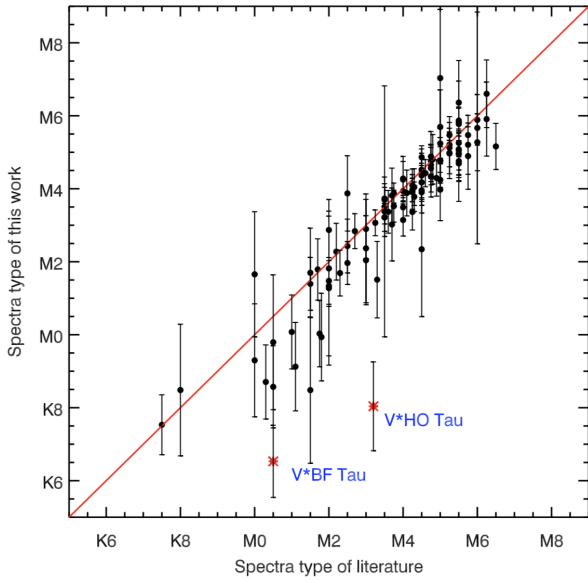


Figure 6. The comparison of the spectral types between the literature (Wichmann et al. 1996; Slesnick et al. 2006; Kraus et al. 2017; Luhman 2018) and those derived from LAMOST spectra in this work. Red asterisks denote the two variable stars HO Tau and BF Tau.

100 Myr isochrone from PARSEC (Bressan et al. 2012). The derived extinctions are consistent with the above ones using the model colors for the 10 Myr isochrone from PARSEC. The J -band extinction of each source used in this work is listed in Table 1.

4. RESULT

4.1. The ages of groups

In Figures 8 and 9, we show the dereddened M_{GRP} vs $G_{BP} - G_{RP}$ color-magnitude diagrams (CMD) of individual groups identified in Section 3. We fit the dereddened M_{GRP} vs $G_{BP} - G_{RP}$ diagrams with the model isochrones of the PAdova and TRieste Stellar Evolution Code (PARSEC, Bressan et al. 2012)². The best-fit isochrone for each group is achieved by minimizing the mean distance of its member candidates to the isochrones. The age of the best-fit isochrone is adopted as the age of the group. From the fitting, 8 groups (Groups 1-8) have ages of 2–5 Myr, while the other 14 groups have ages ranging from 8 to 49 Myr.

In 6 young groups, Group 2, 3, 4, 6, 7, and 8, we have found 47 new member candidates in total. We note that many of them locate below the best-fit isochrone for each young group and could be contaminants from "older" populations in the field. This can be even clearer in Fig-

ure 10 where we plot the 47 member candidates together in the dereddened M_{GRP} vs $G_{BP} - G_{RP}$ diagram. In the figure, about 50% of them locate near the 100 Myr old isochrone. In this work, we only include the ones above 10 Myr old isochrone as the probable members of young groups. This criterion is defined as a compromise between reducing the contamination from the "older" populations and the large spreads in the dereddened M_{GRP} vs $G_{BP} - G_{RP}$ diagrams for young groups. According to this criterion, we include the 17 sources as the members of the young groups, 13 of which are in Group 7, and exclude 30 the other ones in the further analysis and discussion.

After excluding the contamination, we re-fit the dereddened M_{GRP} vs $G_{BP} - G_{RP}$ diagrams of the 5 young groups using the PARSEC isochrones. For Groups 2, 3, 6, 8, we derive the similar ages as before, and for Groups 4 and 7, we obtain the younger ages than before, 2 Myr vs. 3 Myr, and 3 Myr vs. 5 Myr. After excluding the contaminants, in Figures 8 we can still see that some sources are located below the best-fit isochrones and look like old populations. All these sources are known young stars in the literature and harbor disks (see Section 4.2). The locations of these sources in CMDs could be due to accretion activities, the disk orientation, etc. (Fang et al. 2020b). Compared with the young groups, the "old" groups show well defined loci in the CMDs, and their ages can be constrained very well with the PARSEC isochrones. The age of each group is listed in Table 2.

We also fit the observed M_{GRP} vs $G_{BP} - G_{RP}$ diagram using the PARSEC isochrones with an assumption that all member candidates of each group have the same extinction³. As a comparison, the ages of the best-fit isochrones are also listed in Table 2. In general, the ages estimated in two ways are consistent with each other.

We verify our age estimate using the strength of the Li I absorption line at 6708 Å which is a good indicator of stellar ages (Soderblom et al. 2014). In Figure 11, we show the Li I absorption line in the LAMOST spectra of the sources with spectral types around M3. Although the spectral resolution is relative low ($R \sim 1800$), we can clearly see the rapid Li depletion around 10-30 Myr for the M3 type young stars, which is consistent with the results in the literature (see Zuckerman & Song 2004 for a review).

4.2. Circumstellar disks

² Notice that, in the isochrone fitting process, only stars with the flux errors in G_{BP} and G_{RP} bands less than 10% are included.

³ Noted the assumption on the extinction may be improper for the young groups where the extinction from circumstellar material and its parental cloud vary from star to star.

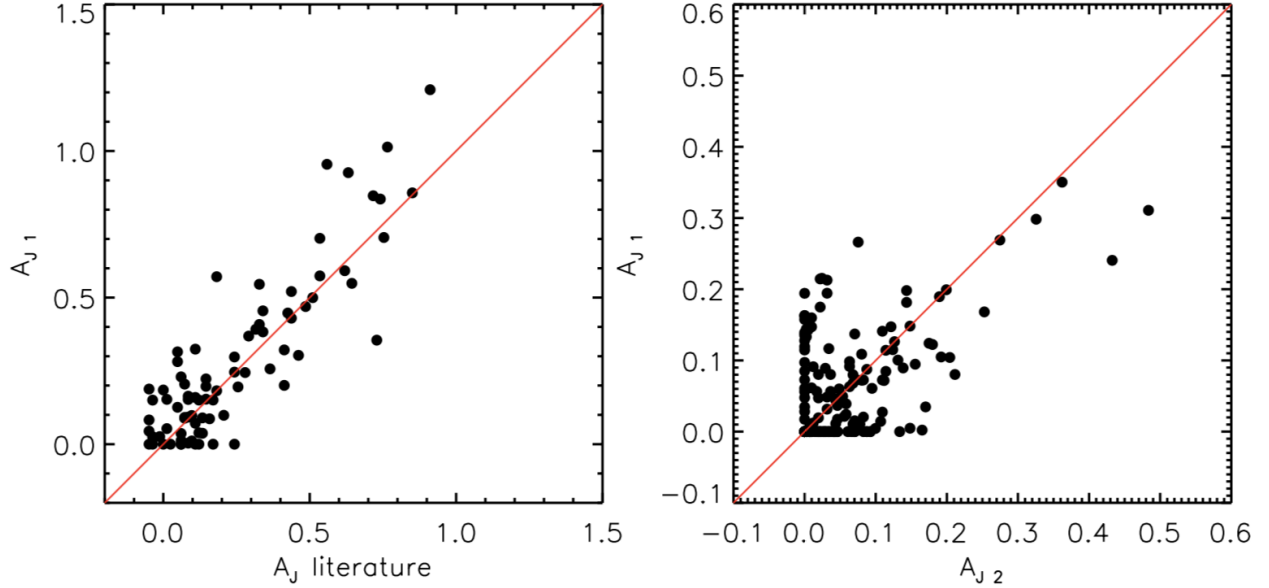


Figure 7. The extinction comparison. The left panel shows the comparison between the extinctions derived from the method we applied to stars with spectral types (A_{J1}) and the literature (Herczeg & Hillenbrand 2014). Right panel is the comparison of the extinctions derived from the two methods of this work (A_{J1} derived from the method we applied to stars with spectral types, while A_{J2} for method of no spectral types). The target stars are members of comparatively older groups (age ≥ 5 Myr) that with known spectral types. The red solid line shows the 1:1 relation.

In this work, we use the infrared photometry from *2MASS* and AllWISE Catalog to search for the objects with disks. In both the catalogs, we extract photometry for 609 common stars. In Figure 12, we show their infrared color-color diagrams used to identify the sources with disks. In the figures, the stars to the bottom-right side of the reddening vector are too red to be explained by the reddening of diskless stars, suggesting there are substantial excess emission above the photospheric level in these wavelengths, which is most likely due to emission from the disks surrounding them. Thus, we identify these sources as stars with disks. In this way, we identify 123 reliable disk-bearing sources (see Figure 12), including 104 known ones confirmed in the literature (Maheswar et al. 2002; Rebull et al. 2011; Eisner et al. 2004; Esplin et al. 2014; Menu et al. 2015; Esplin & Luhman 2019)⁴. We compare our disk classification with the result in Esplin & Luhman (2019), and notice that we have missed 20 disk-bearing stars. Among them, 14 ones only show the infrared excess emission in *WISE* W4 band or the Spitzer 24 μm band, and thus are not identified in

⁴ Among the 104 sources, Sources 595 and 596 are two A-type stars belonging to one binary system (A2+A7) with a circumstellar disk around the A2-type star, Source 596 (Dunkin & Crawford 1998).

this work⁵. Among the other 6 sources, three of them (Sources 63, 250, and 255) can not be cross-matched with the sources in the ALLWISE catalog within $2''$. Another two stars (Sources 19 and 118, red rectangles in Figure 12) locate near the boundary in the left two panels in Figure 12 which we use to identify the sources with infrared excess emission, and might have weak infrared excess emission in those *WISE* bands. Unfortunately the two sources have no photometry in *WISE* W3 band. For the reminding one source (Source 91 or V710 Tau A), it is one component of a binary system (V710 Tau), and the *WISE* data cannot resolve the system. In this work, we list the 20 sources as harboring disks in Table 1. The other 19 disk-bearing sources are firstly revealed in this work. In Figure 13, we show the spectral energy distributions (SED) of these sources. Among these sources, 8 are in young groups (Groups 6, 7 and 8). Interestingly, we also find 11 disks in the relatively older Groups (8 to 11 Myr), 2 in Group 9, 4 in Group 10, and 5 in Group 11.

4.3. Accretion

Classical T-Tauri Stars (CTTS) and Weak-Line T-Tauri Stars (WTTS) can be distinguished from the H α emission (White & Basri 2003). CTTSs usually show

⁵ The photometry in Wise W4 band is not used to identify the disk-bearing star in this work.

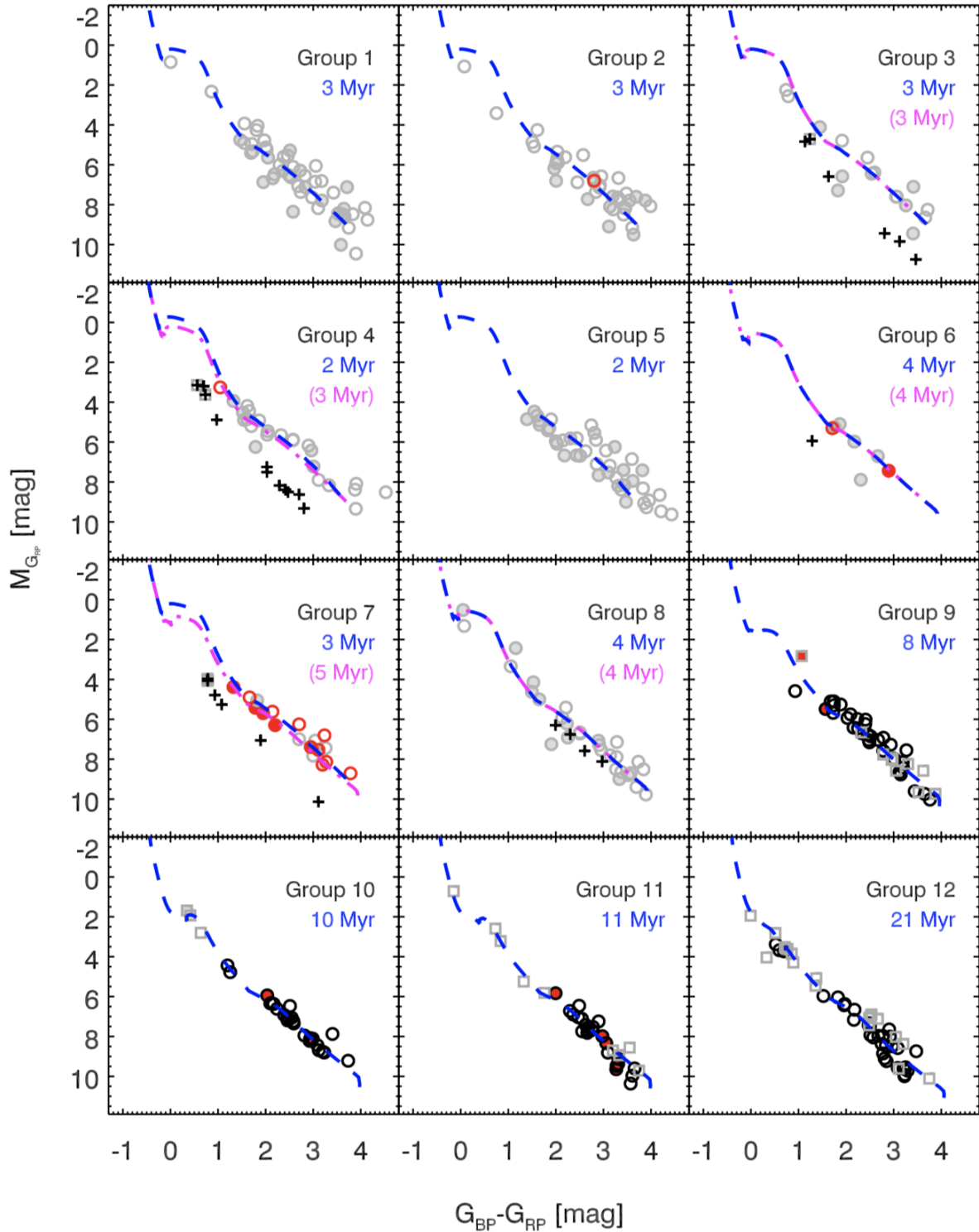


Figure 8. Best-fit isochrones (blue dashed lines) for the stellar groups 1–12 in dereddened $M_{G_{RP}}$ vs $G_{BP} - G_{RP}$ diagrams. The purple dashed-dotted lines in the panels of group 3, 4, 6, 7 and 8 denote the isochrone fit result without removing the contamination of field stars. New identified YSOs and disk bearing stars of this work are denote as red open circles and red filled circles respectively. Gray open circles are YSOs catalogued by [Esplin & Luhman \(2019\)](#), while the gray rectangles show the known intermediate-age PMS stars in the literature (e.g. [Slesnick et al. 2006](#) and [Kraus et al. 2017](#)). The disk-bearing stars confirmed by [Esplin & Luhman \(2019\)](#) are denote as gray filled circles. Black crosses mark the likely contaminants of field stars.

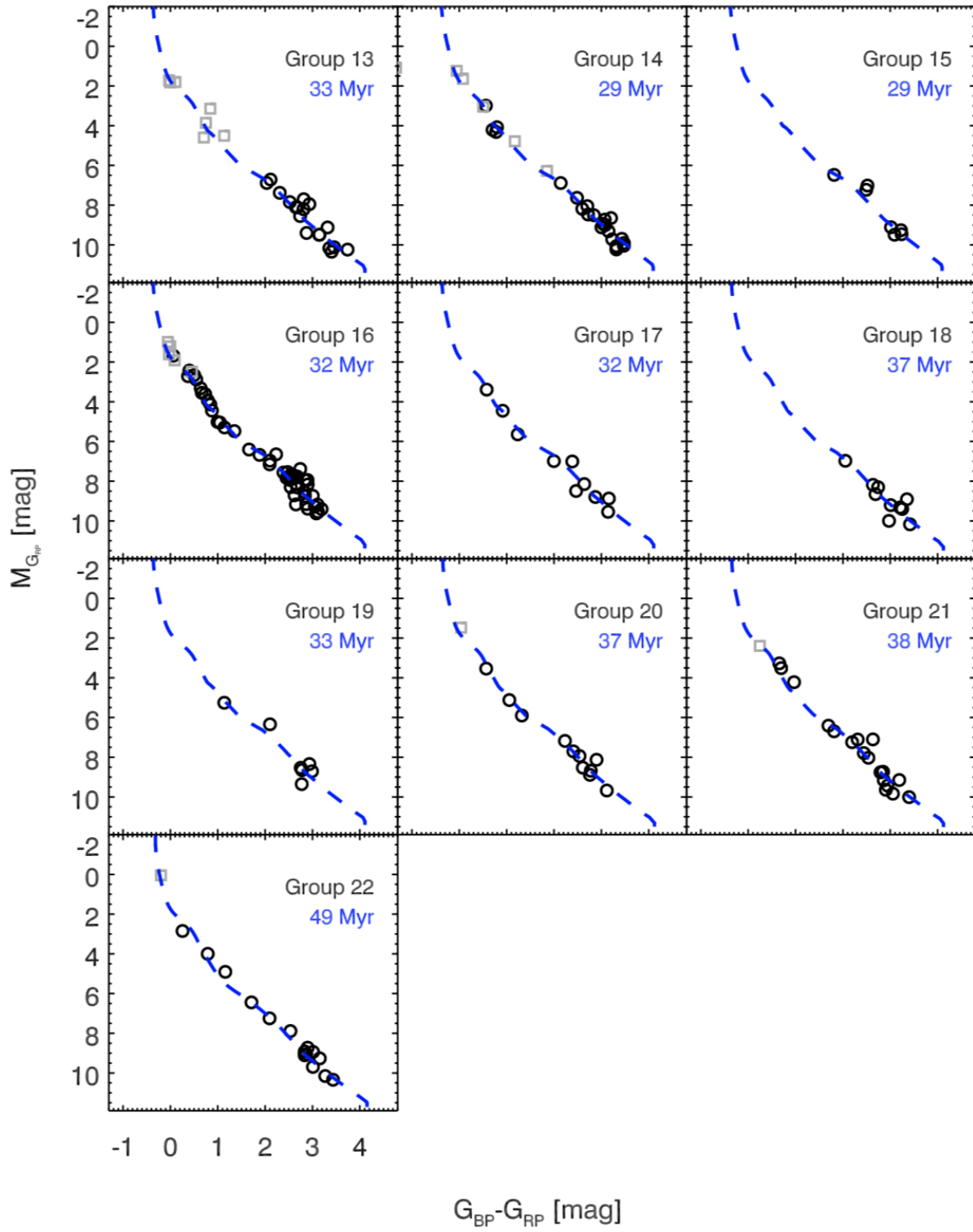


Figure 9. Same as figure 8, but for Groups 13-22.

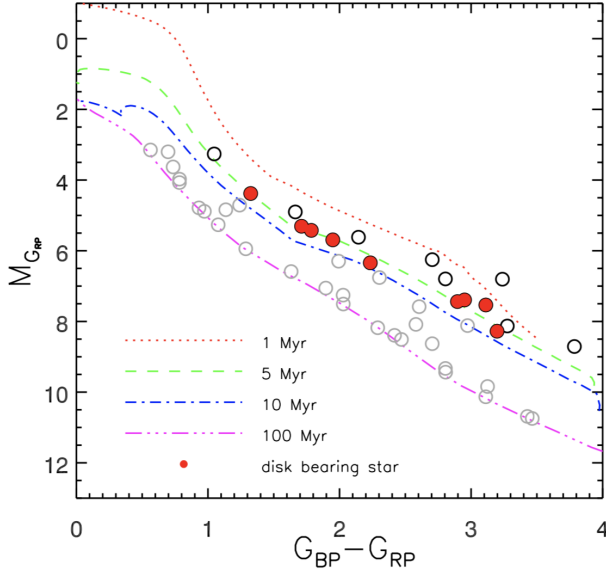


Figure 10. The dereddened $M_{G_{RP}}$ vs $G_{BP} - G_{RP}$ diagrams for the newly discovered member candidates (black open circles for those without disks and red filled circles for those with disks) in young groups. The gray open circles show the sources with ages old than 10 Myr and are excluded as the members of young groups. The isochrones are taken from the PARSEC models.

strong and broad $H\alpha$ emission line due to the accretion process, and WTTSs present weak and narrow $H\alpha$ emission line due to the chromospheric activity. In this work, we use the criteria from Fang et al. (2009) to divide the stars with LAMOST spectra into WTTSs and CTTSs based on their $H\alpha$ equivalent widths (EW_s). Among the 224 stars with $H\alpha$ emission in their spectra, 38 are CTTSs. The results are listed in Table 1 (column 11). Among the CTTSs, 37 sources are in the groups with ages younger than 5 Myr, and one (Source 332) is in Group 10 at an age of 10 Myr (see the discussion in Section 5.2).

In the relative older groups, we discover 11 sources with circumstellar disks, see Fig. 13. Among the 11 sources, we have LAMOST spectra for 4 of them, Sources 331 (Group 10), 332 (Group 10), 355 (Group 11) and 368 (group 11). Based on their $H\alpha$ EW_s , Source 331, 355 and 368 are classified as WTTSs and Source 332 is a CTTS. The $H\alpha$ EW of Source 332 is about -53 \AA , which is much stronger than the threshold (-18 \AA) used to distinguish CTTSs from WTTSs. Figure 14 compares its $H\alpha$ line with that of a WTTS star (Source 374) with a similar spectral type. The $H\alpha$ line profile of Source 332 is well resolved in the LAMOST spectra. We fit its $H\alpha$ line profile using a Gaussian function and derive the full width of half maximum ($FWHM$) of 243 km s^{-1} . With an assumption that the

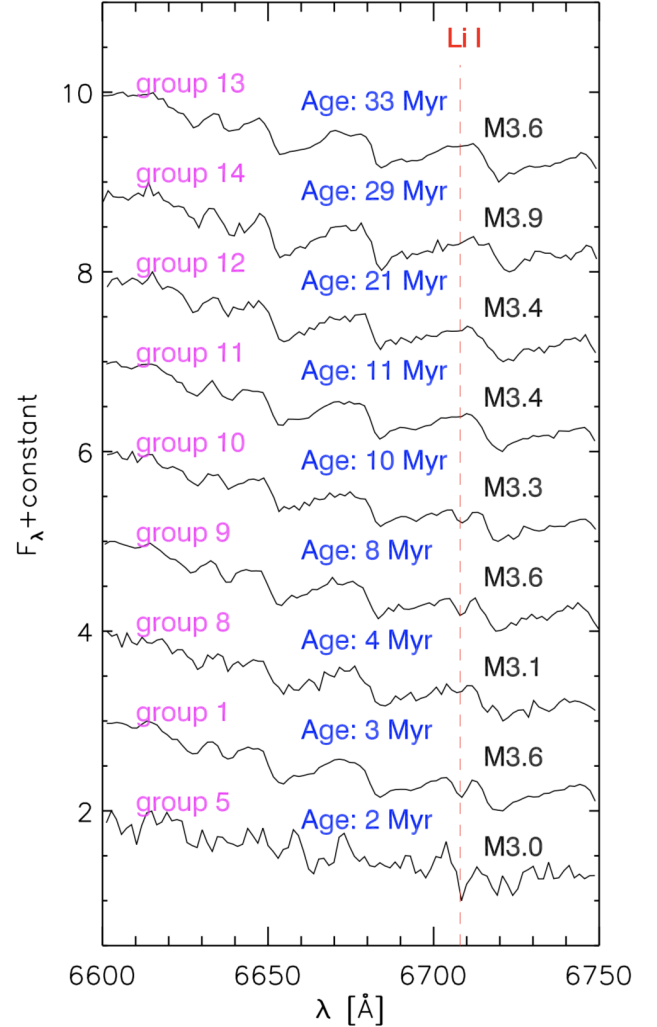


Figure 11. LAMOST low-resolution spectra for \sim M3–M4 type stars at different ages. The red dashed line denotes the Li I 6708 \AA line.

intrinsic $H\alpha$ line profile is a Gaussian function and after deconvolved from the spectral resolution ($R \sim 1800$), the intrinsic full width at 10% maximum ($FWHM_{10\%}$) of the line profile is 343 km s^{-1} , which gives an accretion rate of $\sim 3 \times 10^{-10} M_{\odot} \text{ yr}^{-1}$ using the relation between the $FWHM_{10\%}$ and accretion rates from Natta et al. (2004). Source 332 shows a SED, typical for an evolved disk, with no infrared excess in WISE-W1 and W2 band, and weak excess emission in WISE-W3 and W4 bands. Thus, we might witness the accretion process at the latest stage of disk evolution.

5. DISCUSSION

The ages of our groups range from 2 to 49 Myr. According to their ages, we divide them into two categories: young Groups (2–4 Myr) and old groups (8–49 Myr). A

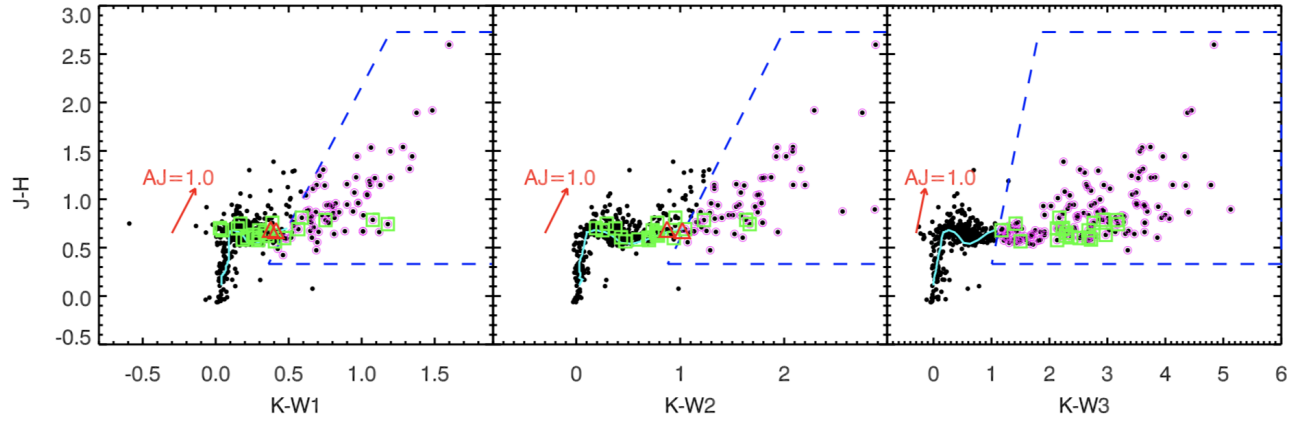


Figure 12. Color-color diagrams for the members (black dots) of all the groups identified in this work. Cyan solid curve in each panel shows the intrinsic colors of PMS stars from [Pecaut & Mamajek \(2013\)](#), while red arrow denotes the extinction vector of $A_J = 1.0$ mag. Purple open circles in each panel display the sources with infrared excess emission in the used WISE band in that panel, and the green boxes mark the 19 disk-bearing stars newly identified in this work. The two disk bearing stars which are not confirmed in this work due to the lack of W3 band photometries are marked as red rectangles.

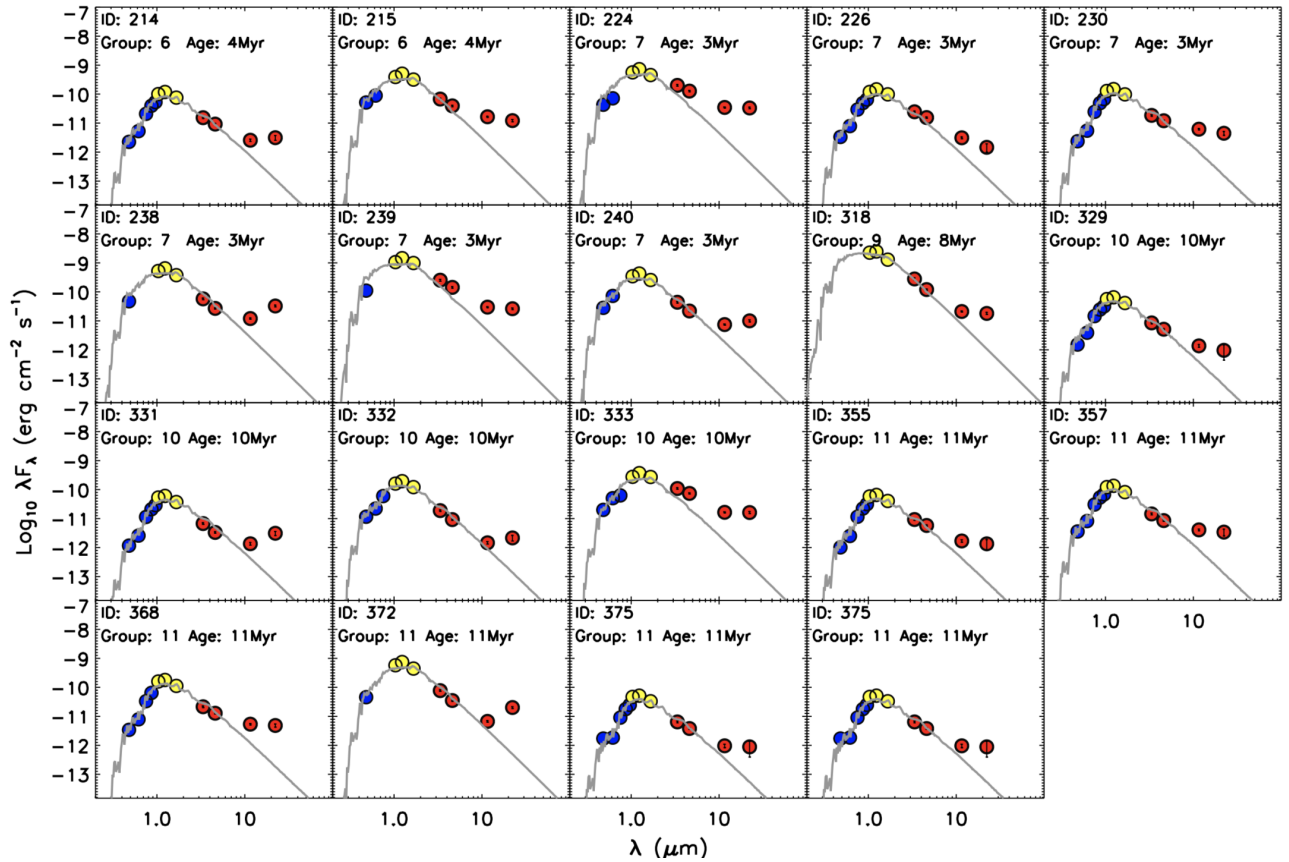


Figure 13. The SEDs of the 19 newly discovered disks. Blue solid circles denote the photometries of Pan-STARRS (The Panoramic Survey Telescope & Rapid Response System, [Chambers et al. \(2016\)](#)), while yellow and red solid circles indicate 2MASS and ALLWISE bands respectively. In each panel, the gray line indicates the photospheric emission level.

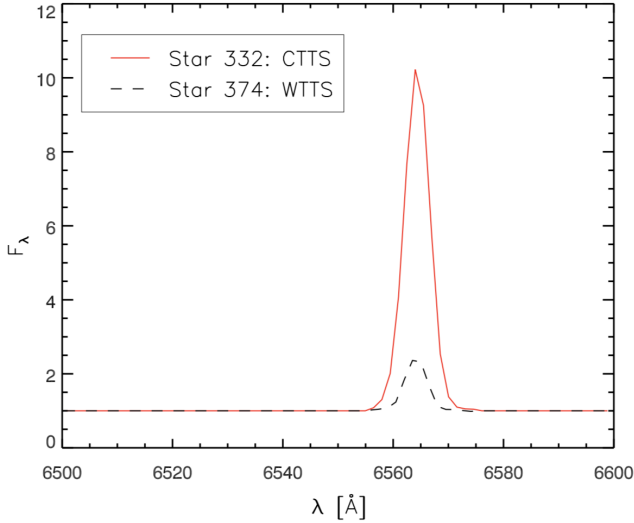


Figure 14. The H α emission comparison between Source 332 (red solid line) and a WTTS star (Source 374, black dashed line) of same spectral type.

discussion of these groups and their relevance to the results in the literature is as follows.

5.1. The Young Groups of this work

In this work, we identify 8 groups, Group 1-8, with ages younger than ~ 4 Myr. Among them, Group 7 have the largest members newly identified in this work. In this group, there are 19 sources and 13 are new. In Group 7, we have 7 M4–M5 type YSOs with LAMOST spectra. In Figure 15 we show the Li I absorption line at 6708 Å for 7 sources. As a comparison, we also show one M4.0 type young stars (Source 28) in Group 1 at the similar age (3 Myr) to that of Group 7. The strengths of the Li I absorption lines of the 7 members in Group 7 are comparable to the one of Source 28, see Figure 15. This supports that Group 7 is at the similar age to that of Group 1.

In Group 7, the 6 known members belong to Population cyan in Luhman (2018) or Group C in Roccatagliata et al. (2020). Group 7 locates to the east of Group 8, is at the similar distance and age to this group. Group 8 is also in Population cyan in Luhman (2018) or Group C in Roccatagliata et al. (2020). Thus, there is one possibility that both Groups 7 and 8 belong to the same group and their separation could be due to that we have not corrected for the projection effect in our grouping procedure. We search for the radial velocities (RVs) for the members in Groups 7 and 8 in *Gaia* DR2, and find the values for 3 sources. We correct for the project effect for Groups 7 and 8 employing the method in Kraus et al. (2017). We derive the median values of the UVW velocities for the 3 sources and assume that all the mem-

bers in the two groups share these median values in the UVW velocity space. For a group member, we subtract its measured proper motions with the ones expected at its location. Figure 16 (a) shows the residual proper motions for Groups 7 and 8, and the standard deviations of the residual proper motions for a combination of the two groups are both ~ 1 mas yr $^{-1}$, which are similar to the values of other young groups in the Taurus. Thus, it is very likely that both Groups 7 and 8 belong to the same group.

We further verify our grouping results for the young stars with the results in the literature. Compared with the ones in Luhman (2018), Groups 1 and 5 belong to the red Population in Luhman (2018), Groups 2, 3, 4 are in the blue Population, and Groups 6, 8 and 7 in the cyan Population. In order to compare with the result in Roccatagliata et al. (2020), we cross-match the members of our young groups with the sources which have a probability of higher than 80% of belonging to one of the Groups A-F in Roccatagliata et al. (2020). We find that Group 1 in this work corresponds to Group A, Group 5 to Group B, Group 6 to Group D, Group 4 to Group E, and Group 2 to Group F, and both Groups 7 and 8 to Group C.

5.2. Old Groups

In this work, we find 14 groups, Groups 9-22, with ages ranging from 8 to 49 Myr and distances within ~ 110 –210 pc. The distributions of these groups are shown in Figure 5. In these groups, there are 353 members and 37 have been catalogued in Kraus et al. (2017). In Group 11, there are 33 members and 6 of them are in the 118 Tau group (total 12 members) in Gagné et al. (2018a). The age of 118 Tau is estimated to be ~ 10 Myr in Gagné et al. (2018a), which is consistent with the age of Group 11. Therefore, it is likely that both Groups 11 and 118 Tau are from the same group.

Oh et al. (2017) searched the comoving star pairs by applying a marginalized likelihood ratio test to 3D velocities of stars of *Gaia* DR1 (e.g. TGAS: Tycho-Gaia Astrometric Solution). And they introduced 13,085 comoving star pairs among 10,606 unique stars. By comparing with their catalogue, we notice that about 20 members of the older groups of this work are also catalogued in Oh et al. (2017). In Group 12 (total 52 members), there are 6 sources belonging to the star pair 29 (9 members) in Oh et al. (2017), in Group 14 (total 30 members), 7 sources are in star pair 28 (9 members), and in another four old groups there are 1-3 sources which have been included in the star pairs in Oh et al. (2017), see Table 2 for more details. Excluding the ones overlapped with those in the literature, 7 old groups are discovered in

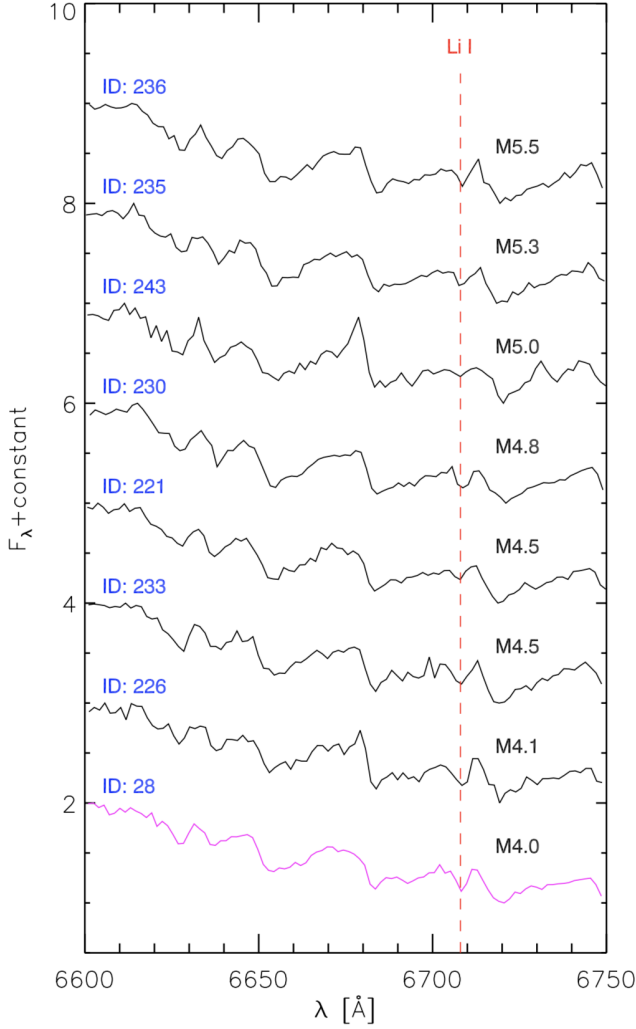


Figure 15. LAMOST spectra for 7 members in Group 7 (black) and one in Group 1 (Source 28, purple). Red dashed line denotes the Li I absorption line at 6708 Å.

this work, including Groups 9, 15, 16, 18, 19, 20, and 21.

We investigate the kinematic relations among the identified YSOs in Taurus and old groups in this work. Similar as done for Groups 7-8, we derive the residual proper motions for Groups 9-22. We adopt the UVW velocities for the identified YSOs from [Luhman \(2018\)](#), and take the median values of them as the common values for the YSOs in Taurus. We derive residual proper motions for the old groups. For Groups 12-22, their residual proper motions are far away from those known Taurus YSOs, indicating that they are not kinematically related to the known Taurus members. Furthermore, these groups are old (>20 Myr) and the Taurus molecular clouds may not be present for so long ([Hartmann et al. 2001, 2012](#)). In Figure 16 (b, c, d), we show the resid-

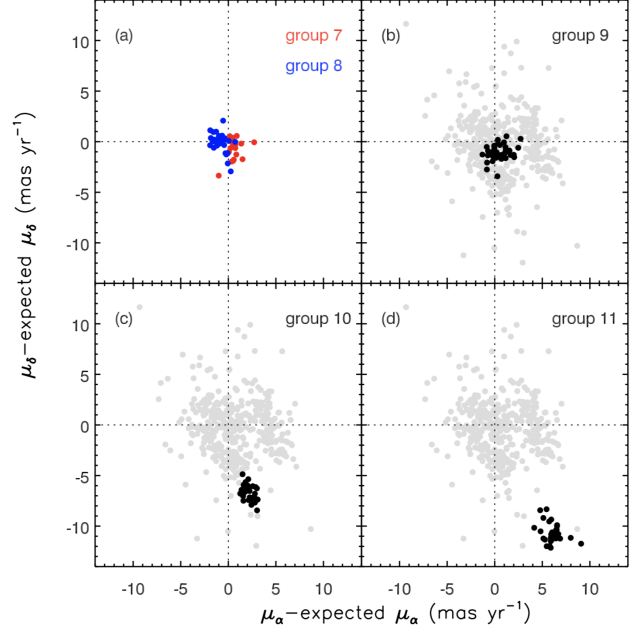


Figure 16. (a) The residual proper motion diagram for Groups 7-8. The residual proper motion for each source is derived by subtracting its measured proper motions with the expected proper motions at its location but with the median space velocities of both groups. (b, c, d) The residual proper motion diagrams for identified YSOs (gray filled circles) and Groups 9-11 (black filled circles). The residual proper motions for individual sources are derived by subtracting their measured proper motions with the expected proper motions at their locations but with the median UVW space velocities of the identified YSOs in Taurus.

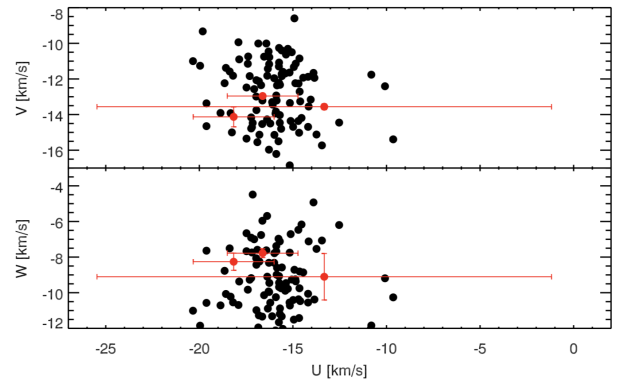


Figure 17. Comparisons of the UVW velocities of three members (red filled circles) in Group 9 with those of the identified YSOs (black solid dots, taken from [Luhman \(2018\)](#)). The typical errors of the UVW velocities for the YSOs are 0.23, 0.18 and 0.12 km s⁻¹ respectively. The uncertainties in the UVW velocities of the members in Group 9 are shown as red error bars.

ual proper motions for the three relative younger groups (Groups 9–11), compared with the identified YSOs. For Group 9, the distribution of its residual proper motions are overlapped with those of known Taurus members, suggesting that there is a kinematic relation between them. In Group 9, there are 4 members (Source 290, 303, 312, 316) with the RVs in *Gaia* DR2. The RV of Star 316 significantly deviates from the other 3 ones, and is thus not used in this work. In Figure 17 we compare the UVW velocities of the 3 sources in Group 9 with those of YSOs in Taurus, which indicates they are kinematically correlated. For Groups 10 and 11, the distributions of their residual proper motions are separated from the YSOs, which excludes that they have any kinematic relations with these YSOs.

6. SUMMARY

In this work, we apply DBSCAN algorithm to the astrometric data of *Gaia* DR2 to search for groups in the Taurus field, and find 22 groups. We derive the ages of these groups by fitting them in color-magnitude diagram with the isochrones of PARSEC models. According to their isochrone ages, the identified groups are divided into two categories: 8 young groups (2–4 Myr), and 14 old groups (8–49 Myr). A summary of the results in this work are listed as follows:

1. Among the young groups, we discover 17 new members. These are newly revealed young stars in Taurus star forming region.
2. Among the 14 old groups, 7 ones, including Groups 9, 15, 16, 18, 19, 20, and 21, are firstly discovered in this work.
3. Using infrared data from 2MASS and WISE, we characterize the disk properties of the sources in the 22 groups, confirm 104 disk-bearing stars in

the literature and discover 19 new ones, 8 of which are in the young groups and 11 are in the 8–11 Myr old groups.

4. We use the strengths of H α emission line to characterize the accretion properties of the group members and discover one star (Source 332) with the accretion activity in 10 Myr old group (Group 10).
5. We find a kinematic relation between Group 9 and the known Taurus members and exclude the relation between Groups 10–22 and the known Taurus members.

We sincerely appreciate the anonymous referee for the instructive advice and productive suggestions. This work is supported by National Key R&D Program of China No. 2019YFA0405501. This work is supported by the National Natural Science Foundation of China (NSFC) with grants No. 11835057 to C. L. and 12003045 to J.M.L.. Guoshoujing Telescope (the Large Sky Area Multi-Object Fiber Spectroscopic Telescope LAMOST) is a National Major Scientific Project built by the Chinese Academy of Sciences. Funding for the project has been provided by the National Development and Reform Commission. LAMOST is operated and managed by the National Astronomical Observatories, Chinese Academy of Sciences. This work has made use of data from the European Space Agency (ESA) mission *Gaia* (<https://www.cosmos.esa.int/gaia>), processed by the *Gaia* Data Processing and Analysis Consortium (DPAC, <https://www.cosmos.esa.int/web/gaia/dpac/consortium>). Funding for the DPAC has been provided by national institutions, in particular the institutions participating in the *Gaia* Multilateral Agreement. Quite a substantial data processing of this work are executed through the software of TOPCAT (Taylor 2005).

REFERENCES

- Bailer-Jones, C. A. L., Rybizki, J., Fouesneau, M., et al. 2018, *AJ*, 156, 58
- Bertout, C., Robichon, N., & Arenou, F. 1999, *A&A*, 352, 574
- Bovy, J. 2014, *Astrophysics Source Code Library*. ascl:1411.008
- Bovy, J. 2015, *ApJS*, 216, 29. doi:10.1088/0067-0049/216/2/29
- Bressan, A., Marigo, P., Girardi, L., et al. 2012, *MNRAS*, 427, 127
- Biazzo, K., Alcalá, J. M., Covino, E., et al. 2012, *A&A*, 542, A115. doi:10.1051/0004-6361/201118379
- Briceño, C., Luhman, K. L., Hartmann, L., Stauffer, J. R., & Kirkpatrick, J. D. 2002, *ApJ*, 580, 317
- Bouvier, J., Barrado, D., Moraux, E., et al. 2018, *A&A*, 613, A63
- Cannon, A. J. & Pickering, E. C. 1993, *VizieR Online Data Catalog*, III/135A
- Cantat-Gaudin, T. & Anders, F. 2020, *A&A*, 633, A99
- Castro-Ginard, A., Jordi, C., Luri, X., et al. 2018, *A&A*, 618, A59. doi:10.1051/0004-6361/201833390

- Chambers, K. C., Magnier, E. A., Metcalfe, N., et al. 2016, arXiv e-prints, arXiv:1612.05560
- Chevance, M., Kruijssen, J. M. D., Vazquez-Semadeni, E., et al. 2020, *SSRv*, 216, 50.
doi:10.1007/s11214-020-00674-x
- Cotten, T. H. & Song, I. 2016, *ApJS*, 225, 15.
doi:10.3847/0067-0049/225/1/15
- Csepany, G., van den Ancker, M., Abraham, P., et al. 2017, *A&A*, 603, A74. doi:10.1051/0004-6361/201527494
- Cui, X.-Q., et al. 2012, *Research in Astronomy and Astrophysics*, 12, 1197
- Dame, T. M., Hartmann, D., & Thaddeus, P. 2001, *ApJ*, 547, 792. doi:10.1086/318388
- Duchene, G., Monin, J.-L., Bouvier, J., et al. 1999, *A&A*, 351, 954
- Dobbs, C. L., Krumholz, M. R., Ballesteros-Paredes, J., et al. 2014, *Protostars and Planets VI*, 3
- Dunkin, S. K., & Crawford, I. A. 1998, *MNRAS*, 298, 275
- Eisner, J. A., Lane, B. F., Hillenbrand, L. A., et al. 2004, *ApJ*, 613, 1049
- Esplin, T. L., Luhman, K. L., & Mamajek, E. E. 2014, *ApJ*, 784, 126
- Esplin, T. L. & Luhman, K. L. 2017, *AJ*, 154, 134
- Esplin, T. L. & Luhman, K. L. 2019, *AJ*, 158, 54
- Ester, M., Kriegel, H., Sander, J., & Xu, X. 1996, *Proc. Second International Conf. on Knowledge Discovery and Data Mining* (Portland, OR: AAAI Press), 226
- Fang, M., van Boekel, R., Wang, W., et al. 2009, *A&A*, 504, 461
- Fang, M., Kim, J. S., Pascucci, I., et al. 2017, *AJ*, 153, 188
- Fang, M., Hillenbrand, L. A., Kim, J. S., et al. 2020, arXiv:2009.11995
- Fang, M., Kim, J. S., Pascucci, I., et al. 2020, arXiv:2011.14483
- Findeisen, K., & Hillenbrand, L. 2010, *AJ*, 139, 1338
- Gagne, J., Mamajek, E. E., Malo, L., et al. 2018, *ApJ*, 856, 23
- Gagne, J., Roy-Loubier, O., Faherty, J. K., et al. 2018, *ApJ*, 860, 43. doi:10.3847/1538-4357/aac2b8
- Gagne, J. & Faherty, J. K. 2018, *ApJ*, 862, 138.
doi:10.3847/1538-4357/aaca2e
- Gaia Collaboration et al., 2016, *A&A*, 595, A2
- Gaia Collaboration et al., 2017, *A&A*, 601, A19
- Gaia Collaboration, Brown, A. G. A., Vallenari, A., et al. 2018, *A&A*, 616, A1
- Green, G. M., Schlafly, E., Zucker, C., et al. 2019, *ApJ*, 887, 93
- Gomez de Castro, A. I., Lopez-Santiago, J., Lopez-Martınez, F., et al. 2015, *ApJS*, 216, 26
- Gudel, M., Briggs, K. R., Arzner, K., et al. 2007, *A&A*, 468, 353
- Guo, Z., Herczeg, G. J., Jose, J., et al. 2018, *ApJ*, 852, 56.
doi:10.3847/1538-4357/aa9e52
- Heintz, W. D. 1975, *ApJS*, 29, 315. doi:10.1086/190345
- Hartmann, L., Ballesteros-Paredes, J., & Bergin, E. A. 2001, *ApJ*, 562, 852. doi:10.1086/323863
- Hartmann, L., Ballesteros-Paredes, J., & Heitsch, F. 2012, *MNRAS*, 420, 1457. doi:10.1111/j.1365-2966.2011.20131.x
- Herczeg, G. J. & Hillenbrand, L. A. 2014, *ApJ*, 786, 97.
doi:10.1088/0004-637X/786/2/97
- Jensen, E. L. N. & Akeson, R. L. 2003, *ApJ*, 584, 875.
doi:10.1086/345719
- Jimenez-Esteban, F. M., Solano, E., & Rodrigo, C. 2019, *AJ*, 157, 78. doi:10.3847/1538-3881/aafacc
- Joncour, I., Duchene, G., & Moraux, E. 2017, *A&A*, 599, A14. doi:10.1051/0004-6361/201629398
- Joncour, I., Duchene, G., Moraux, E., et al. 2018, *A&A*, 620, A27
- Kenyon, S. J., Hartmann, L. W., Strom, K. M., et al. 1990, *AJ*, 99, 869
- Kenyon, S. J. & Hartmann, L. 1995, *ApJS*, 101, 117.
doi:10.1086/192235
- Kervella, P., Arenou, F., Mignard, F., et al. 2019, *A&A*, 623, A72. doi:10.1051/0004-6361/201834371
- Kraus, A. L., Ireland, M. J., Martinache, F., et al. 2011, *ApJ*, 731, 8
- Kraus, A. L., Ireland, M. J., Hillenbrand, L. A., et al. 2012, *ApJ*, 745, 19. doi:10.1088/0004-637X/745/1/19
- Kraus, A. L., Herczeg, G. J., Rizzuto, A. C., et al. 2017, *ApJ*, 838, 150
- Kroupa, P., Jerabkova, T., Dinnbier, F., et al. 2018, *A&A*, 612, A74. doi:10.1051/0004-6361/201732151
- Lada, C. J., & Lada, E. A. 2003, *ARA&A*, 41, 57
- Li, J. Z. & Hu, J. Y. 1998, *A&AS*, 132, 173.
doi:10.1051/aas:1998288
- Liu, J., Fang, M., & Liu, C. 2020, *AJ*, 159, 105
- Lodieu, N., Perez-Garrido, A., Smart, R. L., et al. 2019, *VizieR Online Data Catalog*, J/A+A/628/A66
- Luhman, K. L., & Rieke, G. H. 1998, *ApJ*, 497, 354
- Luhman, K. L. 2004, *ApJ*, 617, 1216
- Luhman, K. L., Mamajek, E. E., Allen, P. R., & Cruz, K. L. 2009, *ApJ*, 703, 399
- Luhman, K. L., Allen, P. R., Espaillat, C., Hartmann, L., & Calvet, N. 2010, *ApJS*, 186, 111
- Luhman, K. L. 2018, *AJ*, 156, 271
- Maheswar, G., Manoj, P., & Bhatt, H. C. 2002, *A&A*, 387, 1003
- Menu, J., van Boekel, R., Henning, T., et al. 2015, *A&A*, 581, A107

- Miroshnichenko, A., Ivezić, Ž., Vinković, D., et al. 1999, *ApJL*, 520, L115
- Muller, P. 1950, *Journal des Observateurs*, 33, 105
- Natta, A., Testi, L., Muzerolle, J., et al. 2004, *A&A*, 424, 603
- Nesterov, V. V., Kuzmin, A. V., Ashimbaeva, N. T., et al. 1995, *A&AS*, 110, 367
- Oh, S., Price-Whelan, A. M., Hogg, D. W., et al. 2017, *AJ*, 153, 257. doi:10.3847/1538-3881/aa6ffd
- Pecaut, M. J., & Mamajek, E. E. 2013, *ApJS*, 208, 9
- Pedregosa, F., Varoquaux, G., Gramfort, A., et al. 2012, arXiv e-prints, arXiv:1201.0490
- Rebull, L. M., Padgett, D. L., McCabe, C.-E., et al. 2010, *ApJS*, 186, 259
- Rebull, L. M., Koenig, X. P., Padgett, D. L., et al. 2011, *ApJS*, 196, 4
- Roccatagliata, V., Franciosini, E., Sacco, G. G., et al. 2020, arXiv e-prints, arXiv:2005.01331
- Scelsi, L., Maggio, A., Micela, G., et al. 2007, *A&A*, 468, 405
- Scelsi, L., Sacco, G., Affer, L., et al. 2008, *A&A*, 490, 601
- Schlafly, E. F., Green, G., Finkbeiner, D. P., et al. 2014, *ApJ*, 786, 29
- Skrutskie, M. F., Cutri, R. M., Stiening, R., et al. 2006, *AJ*, 131, 1163
- Slesnick, C. L., Carpenter, J. M., Hillenbrand, L. A., et al. 2006, *AJ*, 132, 2665
- Soderblom, D. R., Hillenbrand, L. A., Jeffries, R. D., et al. 2014, *Protostars and Planets VI*, 219
- Strom, K. M., & Strom, S. E. 1994, *ApJ*, 424, 237
- Taylor, M. B. 2005, *Astronomical Data Analysis Software and Systems XIV*, 29
- Torres, R. M., Loinard, L., Mioduszewski, A. J., et al. 2009, *ApJ*, 698, 242.
- Wang, S., & Chen, X. 2019, *ApJ*, 877, 116
- White, R. J., & Basri, G. 2003, *ApJ*, 582, 1109
- Wichmann, R., Krautter, J., Schmitt, J. H. M. M., et al. 1996, *A&A*, 312, 439
- Wright, E. L., Eisenhardt, P. R. M., Mainzer, A. K., et al. 2010, *AJ*, 140, 1868
- Zhang, Z., Liu, M. C., Best, W. M. J., et al. 2018, *ApJ*, 858, 41. doi:10.3847/1538-4357/aab269
- Zuckerman, B., & Song, I. 2004, *ARA&A*, 42, 685

Table 1. A list of members in each group

Group ID ^a		Name	RAJ2000 (deg)	DEJ2000 (deg)	Distance (pc)	SpT	Ref ^b	New ^c	Disk ^d	C/W ^e	A _J (mag)
1	1	** KON 2A	67.17759	27.23450	132.4	M5.2	5		5	10.9,W	0.06
1	2	EM* LkCa 4	64.11711	28.12659	129.4	M2	5			3.4,W	0.09
1	3	EM* LkCa 21	65.51311	28.42753	119.9	M2.5	5			5.5,W	0.07
1	4	Gaia DR2 152416436443721728	65.28897	27.84350	117.9	M5.2	5		5	24.8,C	0.13
1	5	HD 28354	67.33263	27.40422	136.7	B9	5				0.00
1	6	HD 283572	65.49520	28.30181	129.8	G4	5				0.12
1	7	IRAS 04171+2756	65.10861	28.06918	127.0	M3.5	5		5	3.9,W	0.06
1	8	IRAS F04147+2822	64.45691	28.49342	128.6	M3.7	5		5	6.4,W	0.41
1	9	J04144739+2803055	63.69748	28.05153	128.2	M5.2	5			4.8,W	0.00
1	10	J04153916+2818586	63.91318	28.31626	131.0	M3.7	5		5	6.9,W	0.44
1	11	J04155799+2746175	63.99167	27.77148	135.2	M5.5	5		5	29.6,C	0.15
1	12	J04161210+2756385	64.05045	27.94403	137.0	M4.7	5		5	7.7,W	0.78
1	13	J04161726+2817128	64.07193	28.28689	130.7	M4.7	5			6.4,W	0.73
1	14	J04161885+2752155	64.07858	27.87094	136.8	M6.2	5			19.0,C	0.50
1	15	J04190110+2819420	64.75460	28.32836	119.0	M5.5	5		5	8.6,W	0.34
1	16	J04201611+2821325	65.06715	28.35903	128.7	M6.5	5		5	45.6,C	0.33
1	17	J04214013+2814224	65.41727	28.23960	127.9	M5.7	5			8.7,W	0.05
1	18	J04230607+2801194	65.77533	28.02210	133.4	M6	5		5		0.21
1	19	J04242090+2630511	66.08707	26.51418	137.2	M6.5	5		5 ^f		0.00
1	20	J04244506+2701447	66.18777	27.02910	126.3	M4.5	5			13.5,W	0.06
1	21	J04251550+2829275	66.31462	28.49098	132.6	M6.5	5				0.00
1	22	J04264449+2756433	66.68540	27.94537	131.8	M6	5				0.14
1	23	J04281566+2711110	67.06528	27.18640	131.3	M5.5	5				0.06
1	24	J04314644+2506236	67.94353	25.10655	131.7	M5.5	5			20.9,C	0.14
1	25	J04315919+2711190	67.99665	27.18863	130.2	M5	5				0.11
1	26	J04372171+2651014	69.34051	26.85042	128.5	M4	5			5.8,W	0.08
1	27	UCAC2 42190684	65.36046	29.87989	127.5	M5.5	5			6.4,W	0.20
1	28	UCAC4 587-012362	68.88191	27.25223	127.4	M4	5			4.9,W	0.03
1	29	UCAC4 588-012108	63.77712	27.47044	133.2	M3.2	5				0.45
1	30	UCAC4 590-012095	64.85502	27.93703	128.5	M3.7	5			5.1,W	0.20
1	31	UCAC4 590-012114	64.95083	27.83353	128.1	M3.2	5			2.9,W	0.03
1	32	USNO-B1.0 1172-00072216	65.16329	27.29216	132.6	M4.5	5			5.4,W	0.00
1	33	V* BP Tau	64.81598	29.10748	128.6	M0.5	5		5	60.6,C	0.11
1	34	V* CW Tau	63.57085	28.18271	131.9	K3	5		5	91.9,C	0.44
1	35	V* CY Tau	64.39053	28.34634	128.4	M2.3	5		5		0.09
1	36	V* DD Tau	64.62970	28.27477	122.8	M3.5	5		5	141.4,C	0.18
1	37	V* FM Tau	63.55660	28.21366	131.4	M4.5	5		5	71.7,C	0.09
1	38	V* FN Tau	63.56081	28.46613	130.8	M3.5	5		5	18.4,C	0.28

Table 1 continued

Table 1 (continued)

Group ID ^a		Name	RAJ2000	DEJ2000	Distance	SpT	Ref ^b	New ^c	Disk ^d	C/W ^e	A _J
			(deg)	(deg)	(pc)						(mag)
1	39	V* IP Tau	66.23784	27.19904	130.1	M0.6	5		5		0.18
1	40	V* V1023 Tau	64.69596	28.33541	125.4	K8	5				0.33
1	41	V* V1070 Tau	64.92195	27.83004	125.9	M0	5			5.4,W	0.01
1	42	V* V1095 Tau	63.30898	28.31963	128.4	M3.6	5			3.6,W	0.11
1	43	V* V1096 Tau	63.36343	28.27351	135.8	M0.5	5			2.5,W	0.53
1	44	V* V1115 Tau	69.07959	25.71639	127.6	K5	5				0.00
1	45	V* V1312 Tau	64.41228	28.55016	129.8	M2.2	5			3.9,W	0.01
1	46	V* V1320 Tau	67.81016	27.17164	127.0	K8	5		5 ^f		0.09
1	47	V* V410 Tau	64.62962	28.45449	130.0	K5	5				0.00
1	48	WK81 1	64.85945	28.43729	131.2	K8	5		5 ^f	3.4,W	0.24
1	49	[BCG93] 1	63.57337	28.10268	135.2	M5	5		5	84.3,C	0.73
1	50	[BCG93] 2	63.77149	28.14613	133.1	M5.5	5			5.8,W	0.26
1	51	[BHS98] MHO 2	63.61001	28.09990	132.3	M2.5	5		5	66.6,C	1.41
1	52	[BLH2002] KPNO-Tau 2	64.71313	28.24258	125.5	M7.5	5				0.20
1	53	[BLH2002] KPNO-Tau 10	64.45649	28.22549	136.9	M5	5		5	44.9,C	0.44
1	54	[BLH2002] KPNO-Tau 11	64.62626	27.72240	129.4	M5.5	5			12.0,W	0.00
1	55	[SS94] V410 X-ray 3	64.53322	28.43435	117.6	M6.2	5		5 ^f	13.7,W	0.05
2	56	Cl* Melotte 25 LH 19	68.80488	17.43049	153.0	M4.5	5			7.6,W	0.16
2	57	Cl* Melotte 25 LH 27	68.74680	17.56057	142.4	M5.7	5			8.8,W	0.20
2	58	Cl* Melotte 25 LH 39	68.57316	17.19201	142.4	M5.5	5			6.6,W	0.08
2	59	Cl* Melotte 25 LH 48	68.42386	17.84448	145.7	M4	5		5	4.2,W	0.25
2	60	Cl* Melotte 25 LH 78	67.67436	17.32855	144.5	M5.5	5			11.7,W	0.17
2	61	Cl* Melotte 25 LH 148	66.14083	15.49291	146.1	M6	5				0.32
2	62	Gaia DR2 3409647134680086784	70.30457	18.22202	140.4	M5.2	5				0.00
2	63	HD 28867B	68.38681	18.01682	149.4	B9.5	5		5 ^f		0.00
2	64	HD 285957	69.66280	15.77044	138.6	K1	5				0.29
2	65	J04285053+1844361	67.21060	18.74337	135.9	M7.2	5		5		0.09
2	66	J04312405+1800215	67.85024	18.00596	144.4	M7	5				0.25
2	67	J04321606+1812464	68.06694	18.21288	144.1	M6	5		5		0.00
2	68	J04322210+1827426	68.09213	18.46185	141.4	M4.7	5		5		0.00
2	69	J04322627+1827521	68.10949	18.46449	147.5	M5.2	5				0.00
2	70	J04324107+1809239	68.17116	18.15665	144.4	M5	5		5		0.00
2	71	J04333278+1800436	68.38670	18.01211	146.6	M1	5		5		0.27
2	72	J04355568+1707395	68.98201	17.12773	142.3	M4.7	5				0.16
2	73	J04360131+1726120	69.00547	17.43669	145.0	M3	5		5	30.0,C	0.28
2	74	J04383885+1546045	69.66188	15.76792	138.5	M3	5				0.00
2	75	J04384502+1737433	69.68760	17.62873	147.4	M4.2	5		5	95.1,C	0.00
2	76	J04384725+1737260	69.69691	17.62391	145.1	M5.5	5		5		0.00
2	77	J04404677+1928033	70.19489	19.46756	146.3	M5.5	5			9.7,W	0.12
2	78	J04440164+1621324	71.00684	16.35899	147.2	M6	5		5		0.20

Table 1 continued

Table 1 (continued)

Group ID ^a		Name	RAJ2000	DEJ2000	Distance	SpT	Ref ^b	New ^c	Disk ^d	C/W ^e	A _J
			(deg)	(deg)	(pc)						(mag)
2	79	J04440556+1821301	71.02319	18.35837	151.6				Y		0.11
2	80	J04455134+1555367	71.46396	15.92685	147.4	M2.5	5		5		0.20
2	81	J04480632+1551251	72.02637	15.85699	152.5	M4.5	5		5		0.81
2	82	J04504003+1619460	72.66686	16.32945	141.6	M4.7	5		5		0.00
2	83	L 1551-51	68.03868	17.95630	142.9	K6	5			1.0,W	0.06
2	84	UCAC4 541-009523	68.47022	18.05459	147.3	M5	5				0.21
2	85	UCAC4 541-010153	70.91926	18.17267	148.3	M5.5	5				0.09
2	86	V* DM Tau	68.45306	18.16944	144.5	M3	5		5		0.02
2	87	V* UX Tau A	67.51664	18.23041	139.4	K0	5		5	7.6,W	0.00
2	88	V* UX Tau B	67.51491	18.23041	136.4	M2	5			8.4,W	0.10
2	89	V* V1076 Tau	68.18223	18.04898	150.3	K6	5				0.21
2	90	V* V1321 Tau	68.22182	17.59268	146.2	M2	5		5 ^f	2.2,W	0.18
2	91	V* V710 Tau A	67.99085	18.35965	142.4	M1.7	5		5 ^f	41.9,C	0.19
2	92	V* V710 Tau B	67.99080	18.36054	144.4	M3.3	5			34.7,C	0.13
2	93	V* V826 Tau	68.06600	18.02743	143.6	K7	5				0.10
2	94	VSS XI-2	67.81577	18.33530	141.7	M4.2	5			5.1,W	0.11
2	95	WISE J043431.29+172219.9	68.63037	17.37225	146.8	M4.2	5		5 ^f		0.00
2	96	[RRN96] GG Tau B	68.12616	17.52512	149.5	M5.5	5		5		0.00
3	97	HD 283641	66.20436	26.71956	160.3	K0	5				0.55
3	98	IRAS 04216+2603	66.18575	26.17059	158.9	M2.8	5		5		0.46
3	99	IRAS F04192+2647	65.56986	26.91588	157.0	M1.5	5		5		0.91
3	100	IRAS F04196+2638	65.69951	26.76469	157.0	M1	5		5		0.84
3	101	J04202316+2817510	65.09652	28.29756	170.9	G4	6		N		0.35
3	102	J04202515+2502493	65.10482	25.04708	160.0				N		0.22
3	103	J04202555+2700355	65.10649	27.00987	169.8	M5.2	5		5		0.55
3	104	J04213459+2701388	65.39414	27.02742	166.3	M5.5	5		5		0.66
3	105	J04213965+2649143	65.41520	26.82057	165.7	M6	5				0.42
3	106	J04214447+2730459	65.43532	27.51274	173.8				N		0.00
3	107	J04215482+2642372	65.47843	26.71039	160.6	M5	5			11.0,W	0.42
3	108	J04221644+2549118	65.56849	25.81995	150.8	M7.7	5				0.11
3	109	J04222404+2646258	65.60019	26.77388	162.6	M4.7	5				0.79
3	110	J04224582+2615350	65.69098	26.25973	159.1	K3	6		N		0.00
3	111	J04234368+2511497	65.93201	25.19716	160.3				N		0.19
3	112	J04245021+2641006	66.20919	26.68352	152.6	M5	5				0.54
3	113	J04272467+2624199	66.85284	26.40551	160.5	M3	5				0.42
3	114	UCAC4 583-012436	68.26882	26.56029	156.3	M4	5			6.0,W	1.13
3	115	V* IT Tau A	68.47797	26.22430	161.3	K5	5		5	13.1,C	0.75
3	116	V* V1201 Tau	66.20064	26.72113	161.4	K1	5				0.63
3	117	[BLH2002] KPNO-Tau 3	66.62246	26.40381	155.5	M6	5		5		0.28
3	118	[MDM2001] CFHT-BD-Tau 9	66.11026	26.83063	154.9	M5.7	5		5 ^f		0.36

Table 1 continued

Table 1 (continued)

Group ID ^a	Name	RAJ2000 (deg)	DEJ2000 (deg)	Distance (pc)	SpT	Ref ^b	New ^c	Disk ^d	C/W ^e	A_J (mag)
3 119	[MDM2001] CFHT-BD-Tau 10	65.44296	26.99150	160.3	M5.7	5		5		0.77
3 120	[XCR2012] TrES J042026+281641	65.10787	28.27825	167.8	G2	4	N			0.24
3 121	[XCR2012] TrES J042423+265008	66.09672	26.83566	154.1	M2	5		5 ^f	4.5,W	0.24
4 122	CCDM J04429+2038AB	70.72125	20.62699	156.0	G0	2	N			0.00
4 123	CoKu HP Tau G3	68.97291	22.90250	156.5	M0.6	5				0.51
4 124	EM* LkCa 15c	69.82413	22.35094	158.2	K5.5	5		5		0.07
4 125	HD 284612	69.71727	20.78074	152.6	F5	12	N			0.10
4 126	IRAS 04303+2240	68.32948	22.77616	147.5	M0.5	5		5		0.87
4 127	J04250121+2031491	66.25505	20.53026	157.9			N			0.07
4 128	J04270739+2215037	66.78085	22.25104	160.6	M6.7	5				0.11
4 129	J04274462+2149280	66.93595	21.82445	158.0			N			0.21
4 130	J04280569+2240590	67.02370	22.68306	147.3			N			0.06
4 131	J04293011+2239154	67.37546	22.65428	161.3	M3	5			3.4,W	0.28
4 132	J04312509+2223219	67.85455	22.38941	163.9	M2.4	7	N		1.0,W	0.00
4 133	J04322415+2251083	68.10066	22.85231	154.8	M4.5	5		5		0.29
4 134	J04324938+2253082	68.20574	22.88561	164.7	M4.5	5		5		0.72
4 135	J04330945+2246487	68.28943	22.78017	149.4	M6	5		5		0.82
4 136	J04332621+2245293	68.35925	22.75813	158.6	M4	5		5 ^f		1.69
4 137	J04334886+2230215	68.45363	22.50594	151.9			N			0.18
4 138	J04340590+2224221	68.52462	22.40616	153.7			N			0.13
4 139	J04341099+2251445	68.54581	22.86233	161.0	M1.5	5			3.8,W	0.43
4 140	J04343609+2225143	68.65041	22.42066	166.4	M7	5				0.16
4 141	J04344544+2308027	68.68935	23.13408	166.7	M5.2	5				0.43
4 142	J04345693+2258358	68.73721	22.97659	161.9	M1.5	5		5 ^f	3.4,W	0.43
4 143	J04354203+2252226	68.92515	22.87295	161.4	M4.7	5			9.6,W	0.68
4 144	J04355286+2250585	68.97028	22.84959	155.9	M4.2	5			7.0,W	0.62
4 145	J04355892+2238353	68.99555	22.64313	158.2	K8	5				0.26
4 146	J04363248+2421395	69.13540	24.36102	158.4	M8	5				0.00
4 147	J04373878+2320590	69.41158	23.34970	159.0	F9	6	Y			0.33
4 148	J04401428+2307544	70.05952	23.13181	151.8	M5.5	5			33.2,C	0.20
4 149	J04433183+2141471	70.88265	21.69644	151.8			N			0.00
4 150	J04460711+2158580	71.52963	21.98276	152.3			N			0.00
4 151	JH 112	68.20465	22.88412	163.8	K5.5	5		5		0.77
4 152	TYC 1279-1849-2	70.72092	20.62723	153.0			N			0.13
4 153	UCAC4 568-011305	68.12730	23.48235	151.6	M4.7	5				0.35
4 154	V* CI Tau	68.46673	22.84169	158.0	K5.5	5		5	42.2,C	0.46
4 155	V* FF Tau	68.83710	22.90673	161.1	K8	5				0.49
4 156	V* HO Tau	68.83421	22.53738	160.7	M3.2	5		5	39.7,C	0.24
4 157	V* HQ Tau	68.94722	22.83934	158.2	K2	5		5		0.63
4 158	V* VY Tau	69.82259	22.79816	151.7	M2	5		5	4.8,W	0.15

Table 1 continued

Table 1 (continued)

Group ID ^a		Name	RAJ2000	DEJ2000	Distance	SpT	Ref ^b	New ^c	Disk ^d	C/W ^e	A _J
			(deg)	(deg)	(pc)						(mag)
4	159	[BLH2002] KPNO-Tau 8	68.92433	22.56989	152.7	M5.7	5				0.07
5	160	** CHN 8A	68.92063	24.18580	124.8	M0.5	5	5	10.4,C		0.83
5	161	Haro 6-13	68.06424	24.48322	130.1	M0	5	5	58.7,C		0.53
5	162	IRAS F04366+2555	69.93700	26.03131	136.4	M5	5	5			0.64
5	163	IRAS S04414+2506	71.11309	25.20457	140.5	M7.2	5	5			0.13
5	164	J04293606+2435556	67.40027	24.59877	129.0	M3	5	5	7.5,W		0.53
5	165	J04295950+2433078	67.49795	24.55214	130.7	M5	5	5	271.3,C		0.56
5	166	J04320329+2528078	68.01372	25.46883	130.0	M6.2	5				0.13
5	167	J04321786+2422149	68.07447	24.37081	123.8	M6	5				0.05
5	168	J04322329+2403013	68.09713	24.05041	129.9	M7.7	5				0.00
5	169	J04330197+2421000	68.25822	24.35002	127.9	M6	5				0.51
5	170	J04340619+2418508	68.52581	24.31410	132.3	M8	5				0.00
5	171	J04350850+2311398	68.78548	23.19441	129.5	M6	5				0.11
5	172	J04381630+2326402	69.56790	23.44451	125.5	M4.7	5		6.0,W		0.00
5	173	J04385859+2336351	69.74417	23.60976	126.4	M4.2	5	5			0.45
5	174	J04385871+2323595	69.74465	23.39985	129.0	M6.5	5				0.00
5	175	J04390163+2336029	69.75681	23.60082	127.4	M4.9	5	5	12.0,W		0.00
5	176	J04390396+2544264	69.76650	25.74065	143.6	M7.2	5	5			0.48
5	177	J04390571+2338112	69.77383	23.63646	127.5	M6	5	5 ^f	42.7,C		0.08
5	178	J04390637+2334179	69.77658	23.57165	123.8	M7.5	5				0.00
5	179	J04390940+2324007	69.78918	23.40017	125.2	M1.5	5		1.3,W		0.07
5	180	J04393364+2359212	69.89017	23.98923	126.7	M5	5	5	48.8,C		0.00
5	181	J04400067+2358211	70.00279	23.97252	120.2	M6	5	5	4.4,W		0.20
5	182	J04414565+2301580	70.44021	23.03278	124.3	M4.3	5	5 ^f	4.6,W		0.00
5	183	NAME V830 Tau b	68.29179	24.56202	130.1	K7.5	5		2.7,W		0.11
5	184	UCAC4 567-010904	68.10270	23.36063	131.4	M4.7	5		4.4,W		0.30
5	185	UCAC4 570-011496	68.98727	23.86315	127.0	M5.7	5	5 ^f	12.8,W		0.17
5	186	UCAC4 577-011850	68.94914	25.39544	129.7	M4.5	5		5.6,W		0.14
5	187	V* CX Tau	63.69942	26.80306	127.5	M2.5	5	5	19.2,C		0.06
5	188	V* DH Tau	67.42313	26.54948	134.8	M2.3	5	5			0.16
5	189	V* DI Tau	67.42697	26.54698	134.6	M0.7	5				0.17
5	190	V* DK Tau A	67.68434	26.02354	128.1	K8.5	5	5			0.17
5	191	V* DK Tau B	67.68497	26.02322	138.7	M1.7	5	15			0.44
5	192	V* DN Tau	68.86407	24.24970	127.8	M0.3	5	5	16.1,C		0.13
5	193	V* DO Tau	69.61912	26.18041	138.8	M0.3	5	5			0.11
5	194	V* FT Tau	65.91329	24.93729	127.3	M3	5	5			0.32
5	195	V* FU Tau	65.89746	25.05076	131.2	M7	5	5			0.29
5	196	V* FY Tau	68.12741	24.33260	129.7	M0.1	5	5			0.74
5	197	V* FZ Tau	68.13235	24.33418	129.6	M0.5	5	5			0.85
5	198	V* GI Tau	68.39192	24.35474	130.0	M0.4	5	5			0.26

Table 1 continued

Table 1 (continued)

Group ID ^a	Name	RAJ2000 (deg)	DEJ2000 (deg)	Distance (pc)	SpT	Ref ^b	New ^c	Disk ^d	C/W ^e	A_J (mag)
5 199	V* GK Tau	68.39401	24.35163	128.8	K6.5	5		5		0.33
5 200	V* GM Tau	69.58891	26.15383	137.9	M5	5		5		0.51
5 201	V* GO Tau	70.76282	25.33853	144.0	M2.3	5		5	49.1,C	0.36
5 202	V* HV Tau	69.64704	26.17740	133.5	M4.1	5			8.2,W	0.34
5 203	V* IQ Tau	67.46482	26.11246	130.8	M1.1	5		5	21.7,C	0.21
5 204	V* V1324 Tau	68.98682	23.86807	125.9	M2	5				0.00
5 205	V* ZZ Tau	67.71411	24.70620	134.0	M4.3	5		5	8.9,W	0.13
5 206	[BLH2002] KPNO-Tau 5	67.44031	26.51293	127.9	M7.5	5				0.14
5 207	[BLH2002] KPNO-Tau 13	66.73882	26.10787	132.9	M5	5		5		0.44
5 208	[HJS91] 507	67.33626	26.56123	128.9	M4.2	5				0.12
6 209	** KSA 32A	76.34508	25.52523	171.1	M1.8	5		5	27.5,C	0.01
6 210	J05044139+2509544	76.17249	25.16516	170.0	M3.7	5		5	88.5,C	0.41
6 211	J05063963+2408095	76.66517	24.13597	165.6			N			0.16
6 212	J05071206+2437163	76.80028	24.62121	172.5	K6	5				0.00
6 213	J05080709+2427123	77.02958	24.45342	178.1	M3.5	5		5	4.9,W	0.09
6 214	J05113705+2402178	77.90438	24.03829	175.7	M4.5	7	Y	7	35.6,C	0.12
6 215	J05123423+2558488	78.14264	25.98021	173.6			Y	7		0.20
6 216	V* V836 Tau	75.77750	25.38878	168.8	M0.8	5		5		0.15
7 217	HD 282697	75.64650	32.44905	154.5	G0	9	N			0.00
7 218	HD 282722	75.66353	31.02971	151.4	F8	9	N			0.00
7 219	J05053836+3125408	76.40986	31.42803	154.6			N			0.00
7 220	J05071404+2934017	76.80851	29.56712	159.9			N			0.07
7 221	J05080636+3026233	77.02650	30.43981	157.4	M4.5	5			5.5,W	0.12
7 222	J05091964+2855332	77.33186	28.92587	157.3	M5	5				0.18
7 223	J05095908+3036453	77.49618	30.61261	151.0			N			0.17
7 224	J05110205+2959282	77.75862	29.99117	160.9			Y	7		0.19
7 225	J05110224+2959232	77.75938	29.98978	160.3			N			0.00
7 226	J05111016+3024061	77.79240	30.40172	159.1	M4.0	7	Y	7	10.6,W	0.13
7 227	J05111352+3024574	77.80639	30.41596	159.6			Y			0.06
7 228	J05124745+3025098	78.19771	30.41938	161.1			Y			0.04
7 229	J05142158+3144291	78.58997	31.74143	153.8			Y			0.05
7 230	J05144607+3011585	78.69197	30.19956	151.8	M4.8	7	Y	7	25.1,C	0.14
7 231	J05152007+3056381	78.83366	30.94391	159.9			N			0.00
7 232	J05162629+2954090	79.10956	29.90250	152.4			Y			0.07
7 233	J05184066+3035014	79.66943	30.58372	155.6	M4.4	7	Y		10.2,W	0.00
7 234	TYC 1853-1659-1	76.91095	27.48317	158.1			N			0.08
7 235	UCAC2 42547226	79.67512	30.58361	154.1	M5.1	7	Y		10.9,W	0.00
7 236	UCAC4 603-018364	77.17723	30.44923	154.7	M5.5	5			11.0,W	0.14
7 237	UCAC4 604-017798	77.49905	30.61173	153.4	M4.2	5				0.10
7 238	V* DW Aur	78.60766	30.01728	154.6			Y	7		0.07

Table 1 continued

Table 1 (*continued*)

Group ID ^a	Name	RAJ2000 (deg)	DEJ2000 (deg)	Distance (pc)	SpT	Ref ^b	New ^c	Disk ^d	C/W ^e	A _J (mag)
7 239	V* HO Aur	76.94571	31.33849	160.4			Y	7		0.17
7 240	V* PW Aur	79.61425	30.14714	156.6	M2.0	7	Y	7	57.1,C	0.00
7 241	V* RW Aur A	76.95607	30.40133	162.8	K6	5		5		0.00
7 242	V* RW Aur B	76.95652	30.40143	156.8	K2	5		5		0.00
7 243	WISE J050841.75+311521.9	77.17399	31.25617	152.9	M5.0	7	Y	17	75.8,C	0.18
8 244	HD 30378	72.09476	29.77301	160.6	B9.5	5		5 ^f		0.00
8 245	HD 31648	74.69277	29.84361	161.1	A2	5		5		1.55
8 246	HD 282630	73.90404	30.29864	159.0	K2	5		5 ^f		0.12
8 247	J04451654+3141202	71.31890	31.68898	155.5	M5.5	5		5		0.40
8 248	J04472593+3135512	71.85806	31.59761	153.5	M3.1	7	N		6.1,W	0.07
8 249	J04481348+2924537	72.05622	29.41493	155.4	M1.7	5		5	19.0,C	0.33
8 250	J04485745+2913521	72.23939	29.23112	160.9	M6	5		5 ^f	5.9,W	0.03
8 251	J04552333+3027366	73.84721	30.46015	164.8	M6.2	5				0.37
8 252	J04554046+3039057	73.91860	30.65156	156.7	M5.2	5			8.3,W	0.14
8 253	J04554535+3019389	73.93897	30.32746	154.1	M4.7	5		5		0.17
8 254	J04554757+3028077	73.94824	30.46877	156.2	M4.7	5			8.4,W	0.05
8 255	J04554801+3028050	73.95009	30.46801	164.3	M5.6	5		5 ^f		0.09
8 256	J04554820+3030160	73.95085	30.50443	160.6	M4.5	5				0.14
8 257	J04554969+3019400	73.95709	30.32778	156.0	M6	5		5		0.17
8 258	J04555636+3049374	73.98486	30.82706	153.8	M5	5			5.8,W	0.13
8 259	J04570011+2910593	74.25048	29.18316	164.6	M5	5			5.1,W	0.20
8 260	J04572852+3029107	74.36879	30.48637	156.3	M3.7	5				0.15
8 261	J04575235+2954072	74.46812	29.90197	158.6	M4.5	5			6.3,W	0.25
8 262	J04584681+2954407	74.69509	29.91131	160.0	M4	5		5 ^f		0.29
8 263	J04585189+2935461	74.71623	29.59613	157.8	M5	5			10.5,W	0.11
8 264	J04593087+2847231	74.87864	28.78975	169.6	M5.5	5			12.5,W	0.00
8 265	PSO J074.1999+29.2197	74.19992	29.21983	158.1	M6	5				0.03
8 266	UCAC4 595-014158	71.91723	28.84470	166.1	M1.6	7	N		3.1,W	0.05
8 267	UCAC4 595-014506	72.74443	28.87273	170.3	M3.8	7	N		4.1,W	0.07
8 268	UCAC4 598-014292	72.08872	29.45334	155.8	M1.7	5				0.05
8 269	UCAC4 598-014396	72.30992	29.57652	166.8			N			0.07
8 270	UCAC4 600-015890	74.69291	29.91247	154.8	M4	5			5.7,W	0.00
8 271	V* AB Aur	73.94102	30.55119	162.1	A0	5		5		0.13
8 272	V* DS Tau	71.95248	29.41977	158.4	M0.4	5		5		0.06
8 273	V* GM Aur	73.79576	30.36649	159.0	K6	5		5		0.07
8 274	V* GZ Aur A	75.01298	30.01846	166.2	M1.5	5		5		0.03
8 275	V* SU Aur	73.99744	30.56708	157.7	G2	5		5		0.16
8 276	V* UY Aur	72.94746	30.78710	154.9	K7	5		5		0.24
8 277	[KW97] 20-19	74.76269	30.05009	155.9	M2	5		5		0.06
9 278	J05210330+2514376	80.26380	25.24379	191.2						0.24

Table 1 *continued*

Table 1 (continued)

Group ID ^a	Name	RAJ2000 (deg)	DEJ2000 (deg)	Distance (pc)	SpT	Ref ^b	New ^c	Disk ^d	C/W ^e	A _J (mag)
9 279	J05220937+2509198	80.53911	25.15551	174.5						0.07
9 280	J05223326+2439251	80.63862	24.65703	179.1	M4.7	4				0.17
9 281	J05223346+2439197	80.63943	24.65549	187.3	M4.5	4				0.03
9 282	J05224508+2440433	80.68788	24.67874	176.3						0.17
9 283	J05230197+2428085	80.75820	24.46905	186.2	M4	4				0.10
9 284	J05230899+2411178	80.78747	24.18827	184.9						0.15
9 285	J05231341+2447111	80.80580	24.78641	186.1						0.20
9 286	J05233572+2434422	80.89882	24.57843	182.0						0.12
9 287	J05234996+2435236	80.95820	24.58990	176.8	M6	4				0.08
9 288	J05235152+2422258	80.96469	24.37384	175.7	M3.6	7		4.4,W		0.07
9 289	J05235528+2425078	80.98034	24.41877	192.0	M3.1	7		7.6,W		0.09
9 290	J05244636+2504329	81.19320	25.07583	181.3						0.05
9 291	J05244654+2504357	81.19393	25.07658	171.4						0.23
9 292	J05250763+2307550	81.28180	23.13197	172.3						0.04
9 293	J05250773+2307475	81.28225	23.12986	182.5						0.08
9 294	J05255573+2444480	81.48222	24.74668	173.7						0.03
9 295	J05264208+2510368	81.67536	25.17688	182.4						0.14
9 296	J05265953+2436077	81.74808	24.60215	174.8						0.05
9 297	J05265958+2436112	81.74826	24.60311	170.5						0.00
9 298	J05271601+2504520	81.81673	25.08109	184.0						0.19
9 299	J05273094+2546533	81.87893	25.78149	178.5						0.17
9 300	J05274889+2513462	81.95372	25.22946	179.2						0.17
9 301	J05284269+2447134	82.17787	24.78705	176.8						0.12
9 302	J05284756+2308019	82.19819	23.13382	166.1						0.24
9 303	J05294539+2408268	82.43915	24.14079	162.5						0.01
9 304	J05295790+2433075	82.49116	24.55210	168.8						0.05
9 305	J05310205+2333576	82.75859	23.56603	165.8	M4	4				0.02
9 306	J05310261+2334020	82.76092	23.56724	168.2	M4	4				0.08
9 307	J05311027+2521156	82.79282	25.35433	169.5						0.02
9 308	J05313955+2512483	82.91484	25.21340	177.6						0.00
9 309	J05314419+2344160	82.93414	23.73777	170.1						0.00
9 310	J05320210+2423028	83.00877	24.38414	171.3	M5	4				0.00
9 311	J05320338+2505072	83.01412	25.08534	178.0	M2.7	7		6.0,W		0.12
9 312	J05330619+2429578	83.27578	24.49941	170.8						0.08
9 313	J05344797+2243139	83.69991	22.72053	167.0	M4.2	4		6.2,W		0.01
9 314	J05421899+2213525	85.57913	22.23125	163.0	M1.6	7		3.8,W		0.07
9 315	J05422002+2213481	85.58348	22.23007	162.9	M2.8	11				0.05
9 316	TYC 1850-1655-1	78.44712	24.64995	184.3						0.05
9 317	UCAC2 40477379	81.43718	24.96972	178.5				7		0.24
9 318	V* V1362 Tau	80.54314	24.53578	186.5	G9	8		7		0.20

Table 1 continued

Table 1 (continued)

Group ID ^a		Name	RAJ2000	DEJ2000	Distance	SpT	Ref ^b	New ^c	Disk ^d	C/W ^e	A _J
			(deg)	(deg)	(pc)						(mag)
9	319	V* V1407 Tau	80.24844	24.76817	178.0						0.01
10	320	HD 35187A	81.00487	24.96044	162.3	A7	Maheswar		14		0.00
10	321	HD 36112	82.61470	25.33252	159.5	A8Ve	13		16		0.00
10	322	HD 243314	81.20269	23.58727	163.9	G0	8				0.07
10	323	J05172871+2704304	79.36965	27.07508	162.2	M4.8	7			11.7,W	0.02
10	324	J05185410+2257470	79.72545	22.96307	164.3	M3.3	7			3.7,W	0.10
10	325	J05200364+2311369	80.01519	23.19360	166.6						0.12
10	326	J05214052+2622057	80.41883	26.36827	162.4						0.06
10	327	J05214383+2626441	80.43259	26.44562	165.2						0.10
10	328	J05225976+2536040	80.74903	25.60110	170.3						0.00
10	329	J05232619+2448302	80.85913	24.80840	162.4				7		0.10
10	330	J05233944+2437411	80.91434	24.62813	171.6						0.12
10	331	J05240115+2326559	81.00483	23.44885	153.1	M4.3	7		7	11.7,W	0.21
10	332	J05240794+2542438	81.03308	25.71217	156.9	M3.1	7		7	53.1,C	0.00
10	333	J05243709+2515509	81.15456	25.26411	157.7				7		0.24
10	334	J05245431+2532480	81.22630	25.54667	159.9						0.11
10	335	J05255171+2512404	81.46546	25.21121	155.6						0.04
10	336	J05260207+2628441	81.50867	26.47889	163.8	M3.3	7			5.9,W	0.07
10	337	J05263850+2527597	81.66040	25.46649	157.5						0.00
10	338	J05264941+2507329	81.70592	25.12580	163.3						0.12
10	339	J05272692+2554163	81.86220	25.90455	160.9						0.10
10	340	J05280370+2520023	82.01542	25.33396	161.0						0.08
10	341	J05291032+2610233	82.29349	26.17252	172.2						0.12
10	342	J05291032+2610233	82.29301	26.17316	168.3						0.07
10	343	J05293311+2518294	82.38800	25.30817	151.2						0.13
10	344	J05293314+2518328	82.38811	25.30915	156.7						0.11
10	345	J05294209+2519129	82.42538	25.32027	154.3						0.11
10	346	J05294967+2459465	82.45696	24.99629	160.0						0.09
10	347	J05295427+2424217	82.47616	24.40604	167.2						0.08
10	348	TYC 1850-225-1	79.25889	26.15559	162.1						0.09
10	349	TYC 1855-1051-1	80.43535	26.44522	163.7						0.24
10	350	V* CQ Tau	83.99361	24.74836	162.4	F5IV	13		18		0.00
11	351	* 118 Tau A	82.31874	25.15021	111.3	B9	1				0.01
11	352	1RXS J052355.2+253052	80.97767	25.51328	107.6	K7	4				0.00
11	353	HD 244354	82.76828	23.20966	109.3	G0	13				0.02
11	354	HD 245358	84.21533	23.43483	108.5	G5	4				0.12
11	355	J05241184+2000354	81.04934	20.00981	105.5	M5.1	7		7	13.9,W	0.05
11	356	J05290021+2533478	82.25090	25.56326	106.9	M3.5	7			6.7,W	0.00
11	357	J05291129+2544450	82.29708	25.74581	113.6				7		0.00
11	358	J05294257+2029130	82.42740	20.48691	101.4						0.10

Table 1 continued

Table 1 (*continued*)

Group ID ^a	Name	RAJ2000 (deg)	DEJ2000 (deg)	Distance (pc)	SpT	Ref ^b	New ^c	Disk ^d	C/W ^e	A _J (mag)
11 359	J05305132+2132140	82.71387	21.53724	104.9						0.00
11 360	J05305876+2312256	82.74485	23.20715	109.1						0.01
11 361	J05310138+2313046	82.75580	23.21798	109.5						0.00
11 362	J05320388+2334309	83.01619	23.57525	112.1						0.00
11 363	J05320631+2432135	83.02632	24.53708	107.3						0.06
11 364	J05333627+2102276	83.40118	21.04100	110.3	M4.5	4			7.9,W	0.00
11 365	J05344263+2813002	83.67760	28.21672	108.5						0.04
11 366	J05361898+2242426	84.07909	22.71186	110.3	M4.7	4				0.00
11 367	J05365428+2343499	84.22616	23.73051	107.7						0.03
11 368	J05370072+2330444	84.25301	23.51236	109.7	M4.7	7		7	17.1,W	0.12
11 369	J05373850+2428517	84.41045	24.48104	114.5	M5.2	4			8.7,W	0.00
11 370	J05375339+2038386	84.47249	20.64404	109.0						0.00
11 371	J05383683+2206498	84.65347	22.11382	108.6	M1.7	7			2.5,W	0.00
11 372	J05383962+2721094	84.66511	27.35261	114.3				7		0.18
11 373	J05390093+2322079	84.75391	23.36890	112.0	M6	4				0.00
11 374	J05392382+1842230	84.84929	18.70638	107.7	M3.4	7			6.9,W	0.16
11 375	J05412474+2228338	85.35311	22.47606	107.1				7		0.03
11 376	J05434172+2356326	85.92389	23.94237	109.7						0.09
11 377	J05455070+2252482	86.46128	22.88003	111.1						0.06
11 378	J05455485+2250068	86.47854	22.83520	111.7	M2.3	7			3.7,W	0.04
11 379	J05463283+2240315	86.63678	22.67541	106.6	K6	10				0.15
11 380	J05485121+1929498	87.21338	19.49720	110.9	M3.2	7			4.2,W	0.02
11 381	J05514663+2456291	87.94431	24.94140	108.7	M3.7	7			7.0,W	0.00
11 382	J05524520+2337489	88.18834	23.63025	108.2						0.05
11 383	J05530802+2522136	88.28343	25.37040	108.2	M3.8	7			4.0,W	0.14
12 384	BD+21 584	61.11870	21.93460	120.5	F8	4				0.00
12 385	CRTS J040513.0+220743	61.30449	22.12880	119.4	M2.0	7			1.7,W	0.00
12 386	CI* Melotte 25 LH 100	67.17497	15.56483	115.2	M4.9	7			12.1,W	0.00
12 387	CI* Melotte 25 LH 132	66.48570	16.21906	121.1	M3.3	7			6.6,W	0.00
12 388	CI* Melotte 25 LH 162	65.98757	16.54606	117.0	M3.9	7			4.7,W	0.19
12 389	CI* Melotte 25 LH 169	65.86590	17.04134	116.4						0.00
12 390	CI* Melotte 25 LH 206	65.21974	17.77821	116.6	M4.6	4			9.7,W	0.09
12 391	CI* Melotte 25 LH 279	63.62596	17.71233	117.9	M3.5	4			4.7,W	0.00
12 392	EPIC 210834430	61.30512	20.39349	117.0	M4.0	7			3.4,W	0.20
12 393	EPIC 210879662	62.35967	21.07546	119.3	M0.7	7			3.0,W	0.09
12 394	HD 25161	60.16939	20.41333	120.6	A0	12				0.19
12 395	HD 25737	61.44656	21.20635	117.6	F5	12				0.05
12 396	HD 284149	61.66166	20.30310	117.8	G1	4				0.00
12 397	HD 284208	63.02388	21.06968	126.4	F6	6				0.05
12 398	HD 284266	63.84551	20.73803	119.5	K0	4				0.06

Table 1 *continued*

Table 1 (*continued*)

Group ID ^a	Name	RAJ2000 (deg)	DEJ2000 (deg)	Distance (pc)	SpT	Ref ^b	New ^c Disk ^d C/W ^e	A_J (mag)
12 399	HD 285372	60.85396	17.40724	118.8	K3	4		0.00
12 400	HD 285373	60.84318	17.27419	122.1	F7	6		0.13
12 401	HD 285778	66.79404	17.84518	119.7	G6	4		0.06
12 402	J03583936+1954499	59.66403	19.91384	122.2	M4.0	7	6.4,W	0.21
12 403	J03590986+2009361	59.79108	20.16004	117.4	M4.7	4		0.27
12 404	J03594481+1704458	59.93671	17.07943	118.1	M3.7	7	6.0,W	0.00
12 405	J04002788+2031591	60.11618	20.53311	115.4	M5.7	4		0.00
12 406	J04043936+2158186	61.16405	21.97182	121.8	M3.4	4	5.9,W	0.07
12 407	J04043984+2158215	61.16606	21.97263	122.4	M3.2	4		0.10
12 408	J04053087+2151106	61.37868	21.85295	125.5	M2.7	4	10.5,W	0.02
12 409	J04070891+2223501	61.78712	22.39723	122.7	M4.6	7	8.1,W	0.00
12 410	J04072874+2117031	61.86978	21.28417	118.0	M4.1	7	8.0,W	0.00
12 411	J04073149+2220223	61.88121	22.33955	121.3	M4.0	7	5.5,W	0.06
12 412	J04073502+2237394	61.89590	22.62763	125.1	M4.8	4	10.7,W	0.19
12 413	J04080252+1844167	62.01048	18.73800	119.1				0.02
12 414	J04092432+2104241	62.35140	21.07340	114.6	K7.4	7	1.4,W	0.00
12 415	J04094053+1845089	62.41888	18.75247	119.2				0.24
12 416	J04125503+1652458	63.22937	16.87941	118.5	M4.5	7	7.8,W	0.00
12 417	J04132177+1810241	63.34076	18.17339	122.2	M3.5	4	9.3,W	0.14
12 418	J04135696+2122570	63.48734	21.38248	121.1	M4.7	7	16.6,W	0.00
12 419	J04264240+1638001	66.67670	16.63335	122.1				0.04
12 420	J04273483+1601269	66.89516	16.02416	121.3				0.03
12 421	NAME V* V1069 Tau b	64.71543	17.38794	121.4	K4	4	1.4,W	0.06
12 422	TYC 1262-406-1	61.16446	22.04543	118.5	G0	6		0.10
12 423	UCAC4 531-008793	66.89398	16.02283	119.4	K5	6		0.00
12 424	UCAC4 541-008569	63.33772	18.17965	125.4	M2.6	7	4.8,W	0.00
12 425	UCAC4 541-008742	64.29970	18.12764	125.7	M3.3	7	3.9,W	0.14
12 426	UCAC4 541-008746	64.31344	18.13388	116.9	M3.3	7	5.8,W	0.14
12 427	UCAC4 545-009103	63.81596	18.90497	124.6	M1.2	7	5.1,W	0.14
12 428	UCAC4 548-009379	65.96171	19.54721	119.6	M1.4	7	1.9,W	0.08
12 429	UCAC4 549-009075	64.09142	19.63837	119.2	M3.7	7	10.9,W	0.00
12 430	UCAC4 552-008520	60.95161	20.34004	117.3	M3.3	7	3.6,W	0.00
12 431	UCAC4 554-008751	62.55542	20.71403	120.8	M2.4	7	4.3,W	0.01
12 432	UCAC4 560-008734	61.13400	21.94307	120.1	M1.0	7	2.4,W	0.00
12 433	UCAC4 560-008743	61.20648	21.99452	118.8				0.04
12 434	V* V1307 Tau A	63.21093	19.61603	121.9	K4.5	4	1.1,W	0.77
12 435	V* V1307 Tau B	63.21136	19.61663	124.1				0.00
13 436	CRTS J050358.0+172209	75.99202	17.36929	113.7				0.01
13 437	HD 30633	72.48807	15.53107	116.1	A3	12		0.20
13 438	HD 31281	73.79008	18.44197	121.9	G1	4		0.00

Table 1 continued

Table 1 (continued)

Group ID ^a	Name	RAJ2000 (deg)	DEJ2000 (deg)	Distance (pc)	SpT	Ref ^b	New ^c Disk ^d C/W ^e	A_J (mag)
13 439	HD 31315	73.83154	16.62030	115.1	A0	12		0.00
13 440	HD 31950	75.10133	15.09035	119.5	G5	4		0.00
13 441	HD 32561	76.20857	18.25393	118.8	A2	12		0.13
13 442	J04523806+1536575	73.15855	15.61597	114.0	M4.7	7	4.1,W	0.13
13 443	J04533443+1842212	73.39350	18.70586	122.2				0.07
13 444	J04545474+1718457	73.72808	17.31269	113.0	M3.8	7	4.6,W	0.16
13 445	J04551573+2001480	73.81556	20.03001	117.8				0.01
13 446	J04552978+1615399	73.87409	16.26108	111.9				0.00
13 447	J04561276+1614412	74.05318	16.24478	112.2	M3.3	7	6.2,W	0.16
13 448	J05003003+1723591	75.12515	17.39978	121.4	G5	4		0.33
13 449	J05032480+1649140	75.85335	16.82055	111.1	M4.0	7	6.0,W	0.15
13 450	J05043907+1658327	76.16280	16.97575	113.3				0.00
13 451	J05044989+1815031	76.20785	18.25083	114.2				0.00
13 452	J05050102+1521052	76.25428	15.35145	115.0				0.00
13 453	J05080901+1558524	77.03708	15.98161	123.8				0.00
13 454	J05080950+1616260	77.03963	16.27394	121.7				0.00
13 455	UCAC4 532-010477	74.90387	16.38989	117.3				0.00
13 456	UCAC4 536-011279	75.66821	17.05633	122.6				0.02
13 457	UCAC4 539-011061	74.28446	17.69703	124.4	M3.6	7	5.5,W	0.00
13 458	UCAC4 551-012119	75.69796	20.11257	123.8	M3.6	7	5.4,W	0.11
13 459	UCAC4 552-011796	74.37686	20.23981	121.1				0.00
13 460	V* V1350 Tau	73.94861	17.70059	122.5	K3	4		0.09
14 461	CRTS J043914.3+212123	69.80996	21.35653	125.6	M2.9	7	5.0,W	0.07
14 462	HD 28944	68.61785	23.10924	129.8	F5	12		0.07
14 463	HD 29935	70.97500	22.94441	128.7	A0V	13		0.04
14 464	HD 283818	70.36149	24.17012	131.8	F9	6		0.08
14 465	HD 284494	67.61453	21.95703	126.2	F9	6		0.12
14 466	HD 284496	67.82024	21.84035	125.3	K0	4		1.40
14 467	HD 284658	70.52438	23.06017	122.7	F5	6		0.02
14 468	HD 284659	70.55081	22.94236	123.6	A2	12		0.00
14 469	HD 284761	72.44098	22.39668	125.0	G2	6		0.00
14 470	J04320447+2142189	68.01869	21.70530	125.7				0.02
14 471	J04343452+2306276	68.64384	23.10766	128.9				0.00
14 472	J04361481+2206239	69.06171	22.10666	123.3				0.00
14 473	J04373727+2101358	69.40531	21.02659	114.9	M3.5	7	7.8,W	0.00
14 474	J04385768+2146314	69.74033	21.77540	115.5	M3.7	7	4.3,W	0.16
14 475	J04395073+2133563	69.96137	21.56566	120.7	M6	3		0.00
14 476	J04412508+2240111	70.35451	22.66973	126.3				0.00
14 477	J04420842+2404447	70.53511	24.07907	129.3	M4.5	7	10.3,W	0.03
14 478	J04421502+2142355	70.56262	21.70986	125.2				0.00

Table 1 continued

Table 1 (*continued*)

Group ID ^a	Name	RAJ2000	DEJ2000	Distance	SpT	Ref ^b	New ^c	Disk ^d	C/W ^e	A _J
		(deg)	(deg)	(pc)						(mag)
14 479	J04422038+2121551	70.58493	21.36530	117.9						0.04
14 480	J04423187+1814318	70.63281	18.24218	121.6						0.00
14 481	J04431898+2157039	70.82911	21.95109	122.0						0.04
14 482	J04435302+1825568	70.97092	18.43245	116.0						0.00
14 483	J04462667+1916565	71.61115	19.28237	115.5						0.05
14 484	UCAC4 542-009958	70.27195	18.21814	119.5	M3.4	7		5.9,W		0.14
14 485	UCAC4 549-010352	69.67027	19.74454	117.0	M3.9	7		7.6,W		0.00
14 486	UCAC4 555-010379	69.21873	20.96499	117.5	M4.7	7		9.7,W		0.00
14 487	UCAC4 563-011854	71.27280	22.47663	120.9	M1.5	7		3.1,W		0.05
14 488	UCAC4 565-010679	66.74655	22.96841	124.2				6.7,		0.00
14 489	V* V1117 Tau	69.56506	23.04098	124.8	M1	4		2.3,W		0.09
14 490	V* V1354 Tau	74.37773	20.24155	122.5	K3	4				0.00
15 491	J05414627+2558284	85.44282	25.97460	197.2						0.01
15 492	J05450166+2515134	86.25692	25.25374	204.6						0.09
15 493	J05450169+2515186	86.25702	25.25522	200.6						0.03
15 494	J05452776+2451369	86.36571	24.86025	201.3	M3.9	7		11.1,W		0.00
15 495	J05455454+2700402	86.47725	27.01116	202.4						0.14
15 496	J05463746+2549222	86.65610	25.82280	197.1						0.00
15 497	J05475571+2448265	86.98216	24.80735	205.2	M2.0	7		3.3,W		0.01
16 498	HD 38319	86.49435	23.74742	207.4	A0	8				0.11
16 499	HD 38693	87.10017	20.84958	202.4						0.01
16 500	HD 39285	88.09708	20.69639	198.7	B9V	8				0.03
16 501	HD 39358	88.24254	20.77787	195.6	B9	8				0.01
16 502	HD 39728	88.79058	19.68701	191.2	A0	8				0.00
16 503	HD 247822	87.15154	20.62297	198.9	A3	8				0.00
16 504	J05374821+2330191	84.45092	23.50528	214.1						0.23
16 505	J05381520+2312365	84.56338	23.21011	202.6						0.09
16 506	J05412050+2216217	85.33545	22.27265	205.2	M3.3	7		6.0,W		0.00
16 507	J05422240+2312359	85.59337	23.20996	208.4						0.09
16 508	J05430783+2212394	85.78264	22.21096	210.0						0.01
16 509	J05433787+1900189	85.90781	19.00525	197.2	M3.1	7		9.0,W		0.00
16 510	J05442654+2203542	86.11062	22.06506	207.8						0.10
16 511	J05460835+1925530	86.53481	19.43139	197.0						0.16
16 512	J05462643+2010219	86.61014	20.17274	192.3	K1	6				0.10
16 513	J05473335+2206184	86.88900	22.10514	206.8						0.02
16 514	J05474581+2036447	86.94090	20.61241	180.7						0.13
16 515	J05480236+1950532	87.00988	19.84813	198.4						0.09
16 516	J05490363+2026357	87.26517	20.44326	199.5						0.06
16 517	J05491583+1946415	87.31599	19.77822	199.1						0.01
16 518	J05511191+2017134	87.79966	20.28704	187.1						0.03

Table 1 continued

Table 1 (continued)

Group ID ^a	Name	RAJ2000 (deg)	DEJ2000 (deg)	Distance (pc)	SpT	Ref ^b	New ^c	Disk ^d	C/W ^e	A_J (mag)
16 519	J05512488+1919155	87.85368	19.32095	184.3						0.00
16 520	J05514250+2020236	87.92710	20.33988	199.6	K1	6				0.03
16 521	J05515488+1920446	87.97868	19.34572	199.3	K4	6				0.00
16 522	J05520562+2001453	88.02344	20.02924	177.8	M3.1	7			6.5,W	0.21
16 523	J05523390+1803400	88.14129	18.06112	203.1	M3.2	7			3.8,W	0.22
16 524	J05530177+2039208	88.25739	20.65579	197.6	M2.2	7			4.2,W	0.00
16 525	J05532784+2030299	88.36603	20.50832	201.7						0.00
16 526	J05541881+2048582	88.57839	20.81617	201.1						0.06
16 527	J05541909+2048572	88.57953	20.81589	202.2						0.06
16 528	J05544504+1757024	88.68765	17.95067	205.3						0.06
16 529	J05544905+1904029	88.70439	19.06749	207.3						0.00
16 530	J05551856+1845425	88.82735	18.76181	196.7	M3.5	7			7.1,W	0.17
16 531	J05553270+1954259	88.88626	19.90721	180.7	M3.9	7			5.2,W	0.00
16 532	J05562113+1757586	89.08806	17.96630	207.3						0.01
16 533	J05562503+2016010	89.10432	20.26694	189.8						0.07
16 534	J05571626+2018314	89.31776	20.30873	214.1	K9.3	7			1.9,W	0.06
16 535	J05571853+1828413	89.32724	18.47812	204.4						0.11
16 536	J05571973+2041572	89.33222	20.69924	211.0						0.00
16 537	J05572252+2117139	89.34382	21.28720	200.5	M0.9	7			2.5,W	0.00
16 538	J05573339+1934110	89.38914	19.56973	202.8	M2.6	7			2.8,W	0.13
16 539	J05573462+2016161	89.39426	20.27115	195.8	M1.3	7			5.8,W	0.11
16 540	J05575494+1844470	89.47894	18.74638	198.4	G8	6				0.02
16 541	J05580038+1902108	89.50160	19.03634	197.6						0.00
16 542	J05580752+2008033	89.53132	20.13426	193.8	K9.1	7			6.1,W	0.00
16 543	J05585832+2018073	89.74302	20.30207	203.7						0.06
16 544	J05594006+2211523	89.91696	22.19787	198.9	M3.5	7			6.5,W	0.00
16 545	TYC 1307-379-1	87.97399	20.61879	202.2						0.00
16 546	TYC 1311-1355-1	87.33366	21.37324	211.7	F9	6				0.00
16 547	TYC 1311-2989-1	87.69121	20.96890	208.1	F4	6				0.00
16 548	TYC 1316-2000-1	88.18336	18.05801	194.8						0.03
16 549	TYC 1320-1412-1	88.66283	19.27755	208.5						0.11
16 550	TYC 1324-122-1	88.19268	20.89370	198.1	F3	6				0.03
16 551	TYC 1324-2796-1	88.58188	20.81839	200.1	G3	6				0.00
16 552	TYC 1324-2810-1	88.24160	20.76863	193.1						0.00
16 553	TYC 1324-377-1	89.00051	21.10678	203.3	G2	6				0.00
16 554	TYC 1862-747-1	85.91609	22.98878	204.6	A7V	6				0.00
17 555	J05384874+2502381	84.70310	25.04389	211.7						0.08
17 556	J05402349+2657166	85.09790	26.95458	213.0						0.24
17 557	J05424292+2545070	85.67883	25.75192	211.4	M1.2	7			3.4,W	0.18
17 558	J05424820+2431196	85.70084	24.52211	213.5						0.05

Table 1 continued

Table 1 (continued)

Group ID ^a	Name	RAJ2000 (deg)	DEJ2000 (deg)	Distance (pc)	SpT	Ref ^b	New ^c Disk ^d	C/W ^e	A _J (mag)
17 559	J05453859+2636023	86.41085	26.60063	208.8	M4.9	7		6.8,W	0.00
17 560	J05455466+2556215	86.47780	25.93931	212.5	M2.8	7		4.0,W	0.01
17 561	J05460009+2621394	86.50038	26.36093	208.9	M2.7	7		3.8,W	0.00
17 562	J05463519+2630473	86.64665	26.51315	218.2	G3	6			0.04
17 563	J05472917+2509568	86.87155	25.16576	210.7					0.03
17 564	TYC 1870-557-1	86.01737	26.87187	210.5					0.14
18 565	J04081592+2957443	62.06636	29.96229	166.4					0.24
18 566	J04164886+3125159	64.20360	31.42108	172.6					0.20
18 567	J04171680+3053521	64.32002	30.89782	168.7	M3.8	7		5.6,W	0.00
18 568	J04185836+3158146	64.74319	31.97071	174.0	M3.7	7		7.0,W	0.09
18 569	J04190537+2940545	64.77239	29.68179	175.0	M3.4	7		5.7,W	0.12
18 570	J04201179+3042143	65.04915	30.70398	170.3	K8.1	7		2.6,W	0.15
18 571	J04232278+3149344	65.84495	31.82620	164.4	M3.5	7		4.9,W	0.01
18 572	J04245709+3110477	66.23787	31.17994	165.7					0.23
18 573	J04253975+3111294	66.41565	31.19152	170.3	M3.0	7		8.0,W	0.35
18 574	XEST 28-001	64.52661	29.08388	173.4					0.24
19 575	J04302586+3017223	67.60776	30.28953	182.9					0.24
19 576	J04321310+2956369	68.05463	29.94359	187.3	K9.3	7		2.0,W	0.27
19 577	J04342346+2934407	68.59781	29.57797	184.0					0.24
19 578	J04344714+3107283	68.69644	31.12453	182.5					0.00
19 579	J04371799+2914156	69.32501	29.23767	181.4	M4.0	7		8.3,W	0.30
19 580	J04373267+2815317	69.38617	28.25882	180.9					0.07
19 581	J04410771+2825415	70.28212	28.42818	184.1					0.24
20 582	HD 40368	89.73908	16.37334	178.9	F0	8			0.24
20 583	J05550440+1837101	88.76836	18.61947	186.7					0.01
20 584	J05551345+1829144	88.80606	18.48733	187.8					0.05
20 585	J05552131+1742397	88.83880	17.71103	186.9					0.03
20 586	J05570842+1657460	89.28508	16.96276	187.3					0.00
20 587	J05574091+1721130	89.42047	17.35358	179.5	M2.5	7		5.6,W	0.00
20 588	J05581907+1750507	89.57949	17.84742	188.7					0.00
20 589	J05585350+1659111	89.72296	16.98626	187.4	M1.1	7		2.1,W	0.00
20 590	J05585878+1657511	89.74493	16.96422	183.6					0.00
20 591	J05590095+1631450	89.75393	16.52924	191.1					0.24
20 592	J05590095+1631450	89.75427	16.52868	189.5					0.00
20 593	J05595131+1657348	89.96383	16.95968	187.2					0.06
20 594	TYC 1312-944-1	89.84604	16.37167	182.6					0.09
21 595	HD 38999	87.65078	24.13669	193.9	A5	8			0.06
21 596	HD 248531	88.07257	24.15585	188.2	F6	6			0.00
21 597	J05425019+2413159	85.70915	24.22108	192.4					0.04
21 598	J05432660+2254355	85.86084	22.90984	196.5	K7.8	7		1.9,W	0.08

Table 1 continued

Table 1 (continued)

Group ID ^a	Name	RAJ2000 (deg)	DEJ2000 (deg)	Distance (pc)	SpT	Ref ^b	New ^c Disk ^d	C/W ^e	A_J (mag)
21 599	J05445268+2357215	86.21950	23.95598	190.8	M2.8	7		4.6,W	0.00
21 600	J05450608+2253546	86.27534	22.89848	185.0	M3.0	7		5.1,W	0.06
21 601	J05450877+2535270	86.28658	25.59080	195.8					0.24
21 602	J05471964+2449433	86.83188	24.82868	188.7					0.08
21 603	J05473314+2105395	86.88812	21.09432	182.3	M0.9	7		4.5,W	0.00
21 604	J05474613+2229388	86.94225	22.49412	181.7					0.06
21 605	J05482582+2156122	87.10761	21.93673	186.9	M2.1	7		5.8,W	0.05
21 606	J05484062+2430116	87.16929	24.50323	187.2					0.01
21 607	J05494879+2240398	87.45333	22.67775	186.6	M3.3	7		4.5,W	0.00
21 608	J05501189+2140089	87.54957	21.66916	188.0					0.04
21 609	J05512875+2257100	87.86984	22.95278	182.6					0.07
21 610	J05525631+2456576	88.23463	24.94933	190.8					0.13
21 611	J05545037+2424459	88.70988	24.41273	191.3					0.02
21 612	TYC 1310-2131-1	84.79289	22.12981	186.8	F4	6			0.00
21 613	TYC 1866-1393-1	86.28893	24.97430	191.3	K1	6			0.04
22 614	BD+12 500	55.04150	13.19874	150.1	F7	6			0.31
22 615	J03443526+1257315	56.14697	12.95878	154.9					0.15
22 616	J03463553+1317056	56.64796	13.28519	157.3					0.07
22 617	J03463553+1317056	56.64821	13.28464	153.0					0.06
22 618	J03472334+1533235	56.84731	15.55654	157.7					0.07
22 619	J03472378+1648282	56.84910	16.80783	154.3					0.14
22 620	J03481036+1608419	57.04319	16.14500	159.9					0.03
22 621	J03484419+1213118	57.18420	12.21996	159.0	K7	6			0.00
22 622	J03495031+1440552	57.45967	14.68197	154.8					0.10
22 623	J03500539+1204146	57.52250	12.07071	153.3					0.05
22 624	J03502880+1356125	57.62002	13.93681	149.5					0.12
22 625	J03510528+1431333	57.77198	14.52596	154.9					0.09
22 626	J03511041+1302467	57.79345	13.04626	162.1					0.03
22 627	J03571372+1237366	59.30719	12.62681	160.6					0.05
22 628	TYC 663-362-1	55.24065	13.15096	147.6	G1	6			0.06
22 629	TYC 664-136-1	57.91520	14.79672	159.7					0.00
22 630	V* V766 Tau	57.81613	13.04608	160.8	B9pS	13			0.09

Table 1 continued

Table 1 (*continued*)

Group ID ^a	Name	RAJ2000	DEJ2000	Distance	SpT	Ref ^b	New ^c	Disk ^d	C/W ^e	A_J
		(deg)	(deg)	(pc)						(mag)

^aThe identification numbers of the stars in this work.

^bThe references for the spectral types: 1. Muller (1950); 2. Heintz (1975); 3. Slesnick et al. (2006); 4. Dunkin & Crawford (1998); 5. Esplin & Luhman (2019); 6. from the LAMOST catalog; 7. This work; 8. Cannon & Pickering (1993); 9. Nesterov et al. (1995); 10. Biazzo et al. (2012); 11. Herczeg & Hillenbrand (2014); 12. Gagné et al. (2018b); 13. Kervella et al. (2019)

^cNew members (“Y”) or nonmembers (“N”) of the young groups (2–4 Myr) identified in this work.

^dWhen the sources are identified as having circumstellar disks, the numbers are for the references : 7. This work; 14. Maheswar et al. (2002); 15. Jensen & Akeson (2003); 16. Eisner et al. (2004); 17. Rebull et al. (2011); 18. Menu et al. (2015)

^e“C” denotes CTTS and “W” for WTTS, the value in front of “C” or “W” is the $H\alpha$ EWs derived from LAMOST spectra.

^fThe 20 disk bearing stars of Esplin & Luhman (2019) that not confirmed in this work.

Table 2. A list of the groups identified in this work.

group	members	PK ^a	Other name ^b	RAJ2000 ^c (deg)	DEJ2000 ^c (deg)	pmRA ^c (mas/yr)	pmDEC ^c (mas/yr)	Distance ^c (pc)	Age ^d (Myr)	Age ^e (Myr)	A _J ^c (mag)
1	55	55	A	65.22	27.91	8.68	-25	129 \pm ₁₂ ⁷	3	3	0.21
2	41	40	F	68.88	17.64	12.15	-18	144 \pm ₈ ⁸	3	2	0.12
3	19	19		66.13	26.65	11.16	-17	159 \pm ₈ ¹⁰	3	3	0.57
4	27	26	E	68.69	22.88	9.89	-17	158 \pm ₁₀ ⁸	2	2	0.45
5	49	49	B	68.53	24.79	7.15	-21	130 \pm ₁₀ ¹³	2	2	0.25
6	7	5	D	76.88	25.02	2.78	-17	172 \pm ₂ ⁵	4	6	0.14
7	19	6	C	78.03	30.43	4.00	-25	156 \pm ₄ ⁶	3	5	0.08
8	30	30	C	73.75	30.08	4.54	-24	158 \pm ₅ ¹⁰	4	4	0.18
9	42	10		81.77	24.42	1.53	-18	176 \pm ₁₃ ¹⁵	8	7	0.10
10	30	4	Oh17-211(3/3)	81.33	25.27	3.65	-25	162 \pm ₁₀ ¹⁰	10	9	0.08
11	33	9		84.32	23.31	5.94	-37	109 \pm ₇ ⁵	11	13	0.03
12	52	18	Oh17-29(6/9)	62.90	19.51	3.76	-14	120 \pm ₅ ⁶	21	23	0.05
13	25	7	Oh17-300(3/3) Oh17-3824(1/2)	74.88	17.27	-2.38	-15	117 \pm ₆ ⁶	33	40	0.04
14	30	7	Oh17-28(7/9)	70.03	21.68	-0.45	-15	122 \pm ₈ ⁸	29	29	0.07
15	7	0		86.35	25.57	10.38	-20	201 \pm ₄ ³	29	40	0.03
16	57	5		87.91	20.46	8.46	-19	199 \pm ₂₂ ¹⁴	33	36	0.04
17	10	0	Oh17-456(1/2)	86.01	25.97	9.18	-19	211 \pm ₃ ⁶	31	37	0.07
18	10	0		64.82	30.79	19.57	-25	170 \pm ₅ ⁴	39	49	0.16
19	7	0		68.85	29.55	18.52	-23	183 \pm ₂ ⁴	40	36	0.20
20	13	1		89.48	17.21	8.46	-20	185 \pm ₇ ⁵	42	43	0.05
21	19	1		86.94	23.50	10.27	-21	188 \pm ₇ ⁷	40	46	0.02
22	17	1	Oh17-1099(2/2) Oh17-43(2/6)	57.11	13.84	23.97	-24	155 \pm ₈ ⁶	49	59	0.08

^aNumbers of the stars with known spectral types in the literature (Slesnick et al. 2006; Kraus et al. 2017; Esplin & Luhman 2019).

^b“A”-“F” denote the Groups of Roccatagliata et al. (2020). Oh17 and “Oh17-X(c/t)” indicate Oh et al. (2017) and the star pair of it. “X” denote the name of the star pair, “t” denotes the total members of the star pair, while “c” denotes how many members contains in the catalogue of this work.

^cThe mean position, distance, proper motion and *J*-band extinction of each individual group

^dThe ages of the groups that derived by fitting the dereddened color-magnitude diagrams with the isochrones of PARSEC models. The extinction of each individual star is considered.

^eThe ages derived by fitting the observed color-magnitude diagrams with the isochrones of PARSEC models, but assuming that all members of a group share the same extinction and treating the extinction as a free parameter.